BERICHTE AUS DEM

ZENTRUM FÜR MEERES- UND KLIMAFORSCHUNG

Reihe A: Meteorologie

Nr. 40

The drift buoys experiment

FRAMZY 2008

Ice drift in Fram Strait and relation to atmospheric forcing

Burghard Brümmer, Gerd Müller
Andrea Lammert-Stockschläder, Annika Jahnke-Bornemann

Zentrum für Meeres- und Klimaforschung der Universität Hamburg
Meteorologisches Institut
2009

Berichte aus dem Zentrum für Meeres- und Klimaforschung

Reihe A: Meteorologie

Nr. 40

The drift buoys experiment

FRAMZY 2008

- Ice drift in Fram Strait and relation to atmospheric forcing -

Burghard Brümmer, Gerd Müller
Andrea Lammert-Stockschläder, Annika Jahnke-Bornemann

Meteorologisches Institut

Hamburg 2009

Die "**Berichte aus dem Zentrum für Meeres- und Klimaforschung"** erscheinen in 6 Reihen mit folgendem Inhalt:

Reihe A:	Meteorologie
Reihe B:	Ozeanographie
Reihe C:	Geophysik
Reihe D:	Biogeochemie und Meereschemie
Reihe E:	Hydrobiologie und Fischereiwissenschaft
Reihe Z:	Interdisziplinäre Zentrumsberichte

Alle Beiträge sind unredigiert und geben allein die Meinung des Verfassers wieder. Sie sollen in erster Linie dem sich jeweiligen Thema befassenden Personenkreis als Arbeitsunterlagen dienen und sind oft gleichzeitig Berichte für die Institutionen, die die betreffenden Arbeiten gefördert haben.

Autoren:

Burghard Brümmer, Gerd Müller, Andrea Lammert-Stockschläder,
Annika Jahnke-Bornemann
Meteorologisches Institut, Universität Hamburg
www.mi.uni-hamburg.de

Volltext (pdf): **www.bis.zmaw.de**

ISSN 0947-7128

Zentrum für Meeres- und Klimaforschung der Universität Hamburg
Bundesstr. 53 – 20146 Hamburg

Contents:

Abstract

This paper reports on the field phase of the FRAMZY 2008 experiment which aimed at the measurement of the sea ice drift in the Fram Strait and its relation to the atmospheric forcing, primarily to that by cyclones. FRAMZY 2008 was the fourth experiment with this objective and followed the FRAMZY experiments in 1999, 2002 and 2007. On 20 January 2008, seven CALIB (Compact Air-Launch Ice Buoys) buoys were deployed from a transport aircraft in a regular array of 200 km by 100 km size centered at 82.6° N, 1.0° E in the northern part of Fram Strait. Buoys measured autonomously air pressure, temperature and position at approximately one-hourly intervals and transmitted the data via the Argos satellite system. The lifetime of the buoys before they were lost at the ice edge or due to the breaking of ice was between 7 and 39 days (final date 28 February 2008). The southernmost position reached by a buoy after 39 days was 76.2° N, -12.0° W, corresponding to an average drift speed of 16.9 km per day or 0.20 ms^{-1}. During the FRAMZY 2008 period eight cyclones passed through Fram Strait. The paper presents details of the ice motion and the atmospheric conditions. In the appendix 12-hourly maps of sea-level pressure and surface air temperature as analysed by the ECMWF, daily maps of ice concentration and daily NOAA satellite images are presented.

1. Introduction

The drift buoys experiment FRAMZY 2008 was conducted in January and February 2008. Its main objective was the measurement of the sea ice drift in the Fram Strait and its relation to the atmospheric forcing, primarily to cyclones. This is the reason for the name of the experiment: FRAMZY (Fram Strait cyclones; in German: Framstraßen-Zyklonen).

FRAMZY 2008 was the fourth experiment in a series of FRAMZY experiments with this objective. The first experiment, FRAMZY 1999, took place in April 1999 (Brümmer, 1999), the second one, FRAMZY 2002, in March 2002 (Brümmer et al., 2005), and the third one, FRAMZY 2007, in March/April 2007 (Brümmer et al., 2004). Figure 1.1 displays the site of the FRAMZY experiments. Table 1.1 gives an overview of the experimental periods and of the experimental platforms involved. FRAMZY 2008 was the smallest of the four experiments what the number of platforms concerns: only 7 ice drift buoys were employed. During the preceding experiments in addition to buoys the German research aircraft Falcon was involved and during FRAMZY 1999 and FRAMZY 2002 furthermore the German research vessel Valdivia and the Finnish research vessel Aranda, respectively. FRAMZY 2008, however, was the first experiment which took place in mid-winter. Thus, FRAMZY 2008 enlarges the range of synoptic atmospheric forcing conditions encountered during the preceding experiments.

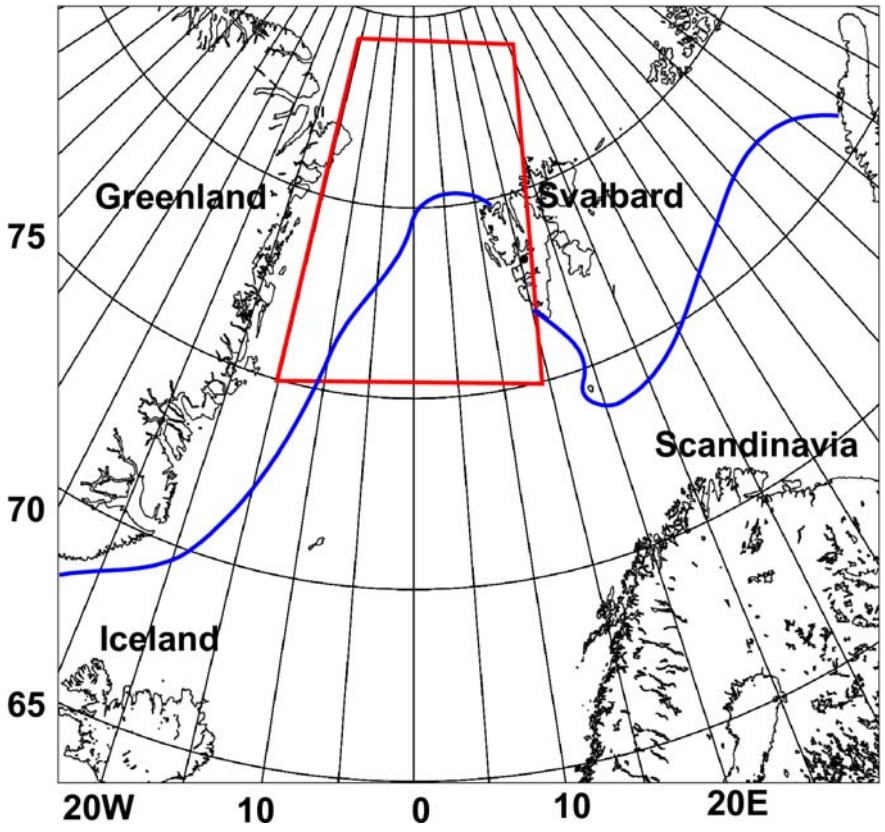

Fig. 1.1: Location of FRAMZY experiments (red box). Blue line marks typical ice edge.

Table 1.1: Overview over all four FRAMZY experiments: period and platforms.

Experiment	Period	Platforms		
		Buoys	**Ship**	**Aircraft**
FRAMZY 1999	03 – 30 April 1999	15 CALIB ice buoys	RV Valdivia	Falcon aircraft
FRAMZY 2002	27 Febr. – 30 April 2002	12 CALIB ice buoys, 2 Ice beacons	RV Aranda	Falcon aircraft
FRAMZY 2007	26 Febr. – 30 April 2007	16 CALIB ice buoys, 13 XAN1 water buoys	-	Falcon aircraft
FRAMZY 2008	20 Jan. – 28 Febr. 2008	7 CALIB ice buoys	-	-

The Fram Strait is a region with a high synoptic activity. This results primarily from the fact that two opposite ocean currents pass through. The West-Spitsbergen current transports warm and salty North Atlantic water northward and keeps the eastern part of Fram Strait ice-free almost the whole year. The East-Greenland current on the western side transports cold and fresh water as well as sea ice from the Arctic Ocean to the Greenland Sea. Thus, strong air temperature contrasts are characteristic for the Fram Strait region, especially in winter. Temperature can change by 20-30 K within a few hours when the airflow reverses from off-ice to on-ice or vice versa. Such extreme airflow reversals are mostly connected with the passage of cyclones and fronts (e.g. Rasmussen et al., 1997; Brümmer and Hoeber, 1999; Brümmer et al., 2003; Brümmer 2005).

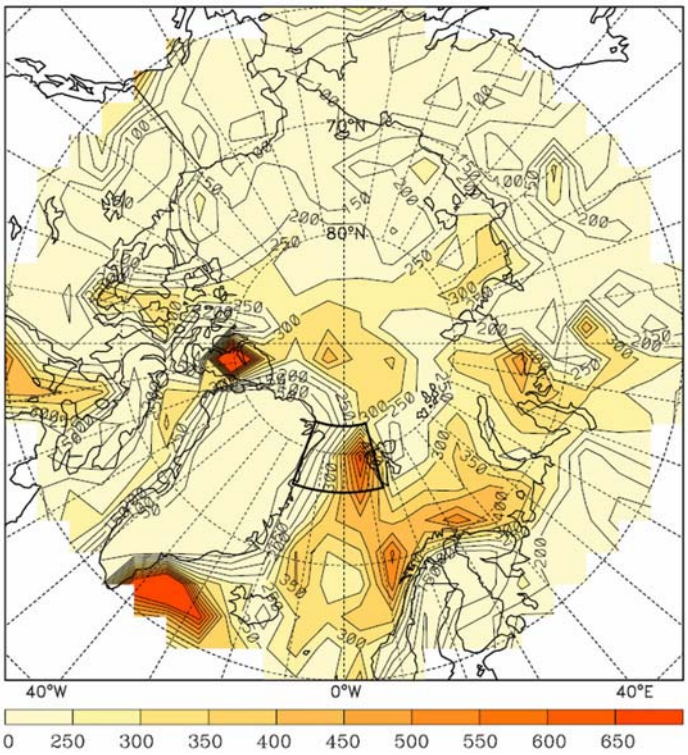

Fig. 1.2: Number of cyclone detections during winter months November-April for period 1978-2000 from European Centre for Medium-Range Weather Forecasts (ECMWF) analyses (from Affeld, 2003). The region of Greenland is clipped out due to its high elevation and uncertainty of pressure reduction to sea level. For the same reason the maximum over Ellesmere Island is probably artificial.

Statistical cyclone studies by Affeld (2003) show that a secondary maximum of cyclone frequency is present over Fram Strait – the primary maximum is situated over the Irminger Sea to the southwest of Iceland, the region where the Islandic low is located (Figure 1.2). According to Affeld cyclones propagate most frequently from southwest to northeast through Fram Strait (Figure 1.3).

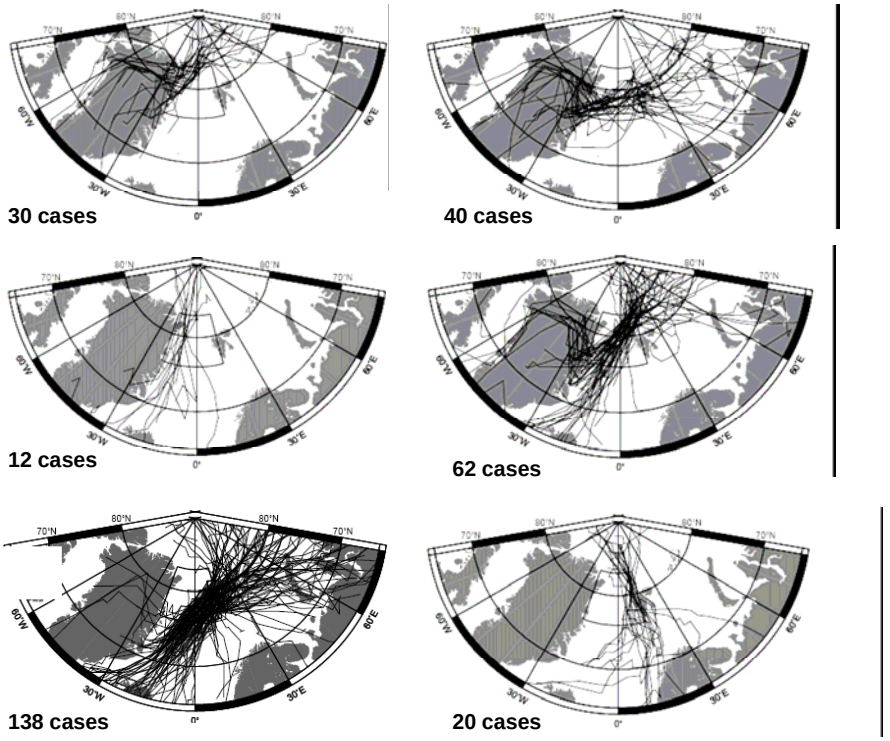

Fig. 1.3: The six most typical cyclone tracks through Fram Strait (from Affeld, 2003)

The impact of cyclones on the sea ice can be manifold. Model and statistical studies by Affeld (2003) and model sensitivity studies by Schröder (2005) show that

- cyclones cause substantial shifts of the ice edge
- cyclones accelerate or decelerate the southward ice drift if their track is more on the eastern or western side of the Fram Strait, respectively.

Numerical sensitivity studies by Kriegsmann and Brümmer (2008) with an idealized cyclone in a coupled ice-ocean model show that a passing cyclone leaves a trail of lowered ice concentration behind it. The degree of ice concentration reduction depends on the cyclone properties (pressure gradient, propagation speed) and on the pre-existing ice conditions (concentration, thickness).

Cyclones can trigger inertial oscillations of the sea ice. Lammert and Brümmer (2008) present an inertial oscillation case observed during FRAMZY 2007. Not all cyclones cause oscillations. A kind of resonant triggering occurs when the propagation speed and the radius of the passing cyclone are such that the changing wind direction is in phase with the changing ice drift direction of the inertial oscillation. Such conditions can occur only on the right side (looking in propagation direction) of the cyclone track. Such a triggering may also happen on

the left side of a passing anticyclone. However, the wind field around anticyclones is mostly weaker.

The mentioned examples show that cyclones can have a direct impact on ice drift (e.g. acceleration or deceleration) and an indirect impact (e.g. ice breaking). The latter impact may change the ratio of ice drift versus atmospheric wind forcing and also the thermodynamic conditions for new ice formation.

Ice drift in Fram Strait is very variable, not only on the synoptic scale but also on the intra-annual and inter-annual time scale. Variations on the latter time scales are primarily connected with the prevailing occurrence of special synoptic conditions. Which are caused by a shift of large-scale pressure patterns such as the Arctic Oscillation (AO), the North Atlantic Oscillation (NAO) or the pressure difference within the North Atlantic low pressure zone between Iceland and Northern-Scandinavia (Jahnke-Bornemann and Brümmer, 2008). Ice export through Fram Strait cannot be determined exactly, but can only be estimated. Estimates are based on data from various instruments and on various methods: satellite data (e.g. Kwok et al., 2004; Spreen, 2008), buoy data (Brümmer et al., 2005), moored upward looking sonar data (Vinje et al., 1998), sea level pressure difference across Fram Strait (Vinje, 2001) or numerical simulations with models of different degree of complexity (uncoupled models, e.g. Harder et al., 1998; coupled ice-ocean models, e.g. Kauker et al., 2003).

The measurements taken during the buoys drift experiment FRAMZY 2008 serve for the following aims:

- process analysis: atmospheric forcing – ice drift
- estimate of ice drift through Fram Strait
- ground truth for satellite-based ice drift retrieval (the temporal resolution of buoy-based drift is much higher than that of the satellite-based drift)
- validation of atmospheric models (is the cyclone correctly analysed/placed?)
- validation of ice models (is the ice drift correctly modelled?)

The report is organized as follows. In section 2 the buoys (type, calibration, accuracy, deployment etc.) are described. In Section 3 summaries of the buoy measurements and the synoptic conditions are presented. Three measurement examples are presented in Section 4: a period with strong northerly flow, a cyclone passage through Fram Strait, and the simultaneous loss of three ice buoys. In the Appendices A1-A3 accompanying information is compiled: 12-hourly operational sea-level pressure analyses, daily ice concentrations, and daily NOAA satellite images.

2. The drift buoys

2.1 Buoy characteristics

The buoys used during the FRAMZY 2008 campaign were so-called Compact Air-Launch Ice Beacons (CALIB) manufactured by METOCEAN Inc., Canada, comprising a pressure sensor (Vaisala PMB-100) and a temperature sensor (YSI Model 44032 Encased Thermistor). The temperature sensor is mounted inside the buoy's tube-shaped housing and, thus, can only be interpreted as "air" temperature with reservation. The temperature represents more or less the near-surface temperature, but it can change to an "inside-snow temperature" if snow covers the sensor package. Buoy data were transmitted via the satellite-based ARGOS system and positions (latitude, longitude) were tracked by ARGOS positioning system. The manufacturer

quotes an absolute system accuracy of ±1 hPa for the pressure measurement and ±1 K for temperature measurement, and ARGOS locations are accurate to about ±300 m. The sensor resolution is 0.1 hPa for pressure and 0.3 K for temperature. The buoys were equipped with Alkaline batteries with a lifetime of at least 3 months.

All sensor data is gathered over the last 12 minutes of a 20 minute period. The data is processed and placed into the new Argos message directly after the sensor sampling period. The sensor data is formatted for ARGOS transmission, and reported information is updated every 20 minutes. At the high latitude of the deployments, the ARGOS system has excellent temporal coverage, and sensor data as well as positions were almost on-line (about one hour after acquisition) via internet available for the user. The pressure and temperature data were not made available on the Global Telecommunications System (GTS) of the World Meteorological Organization (WMO) and thus provide an independent source of information for validating atmospheric model analyses.

The CALIB buoy is 0.92 m long, has a diameter of 0.12 m and a weight of 8.2 kg. The buoy is equipped with a parachute for soft landing on ice and it is not able to swim.

2.2 Buoy calibration before deployment

The buoys were calibrated before deployment to secure the quality of the measurement data. The experimental set up for the buoy calibration is described below.

First the buoys were activated and checked for full functionality. Then, pressure and temperature values were measured simultaneously by all seven buoys and a reference system, Vaisala PTU 200 unit. The calibration took place in a hangar at Longyearbyen airport on Spitsbergen. It started on 18 January 12.26 UTC and ended on 20 January 09.05 UTC. The temperature in the hangar was not constant due to the fact that the door was opened for normal operations. Furthermore, there was a periodic temperature variation due to the hangar heating equipment. Pressure was not affected.

Table 2.1: Means, bias and standard deviations of pressure and temperature measurements of all 7 buoys and the PTU.

B. No.	***Argos No.***	***p buoy [hPa]***	***p PTU [hPa]***	***p Diff [hPa]***	***STD p Diff***	***T buoy [°C]***	***T PTU [°C]***	***T Diff [°C]***	***STD T Diff***
1	73413	1001.28	1000.90	0.37	0.11	14.91	14.81	0.10	0.44
2	73397	1001.16	1000.69	0.53	0.11	14.81	14.80	0.01	0.45
3	73407	1002.17	1001.65	0.48	0.11	14.65	14.81	-0.16	0.42
4	73414	1001.49	1001.01	0.48	0.11	15.32	14.76	0.56	0.52
5	73405	1000.60	1000.08	0.52	0.11	14.49	14.81	-0.31	0.50
6	73406	1001.60	1001.17	0.43	0.12	14.84	14.81	0.03	0.44
7	73398	1002.30	1001.88	0.42	0.11	14.78	14.85	-0.07	0.33
	Mean:	1001.51	1001.05	0.46	0.11	14.83	14.81	0.02	0.44

Results of the calibration measurements are shown in Figures 2.1 and 2.2 and in Table 2.1. During the calibration the pressure increased continuously (Fig. 2.1). A positive pressure offset can be seen for all buoys. There appears to be a weak trend in the pressure offset growing with increasing pressure values. In contrast to pressure, the temperature calibration shows offsets with different signs for the individual buoys (Figure 2.2). A trend of the temperature offset cannot be determined due to the small temperature range. Table 2.1 lists the mean values, the bias and the standard deviations of pressure and temperature for each buoy. The mean pressure bias (buoy minus PTU reference) is 0.46 hPa averaged over all buoys and ranges from 0.37 to 0.52 hPa for the individual buoys. The standard deviations for the individual buoys are around 0.11 hPa. The mean temperature bias is 0.02 K and ranges from -0.31 K to 0.56 K for the individual buoys. The standard deviation for the individual buoy is between 0.33 and 0.52 K.

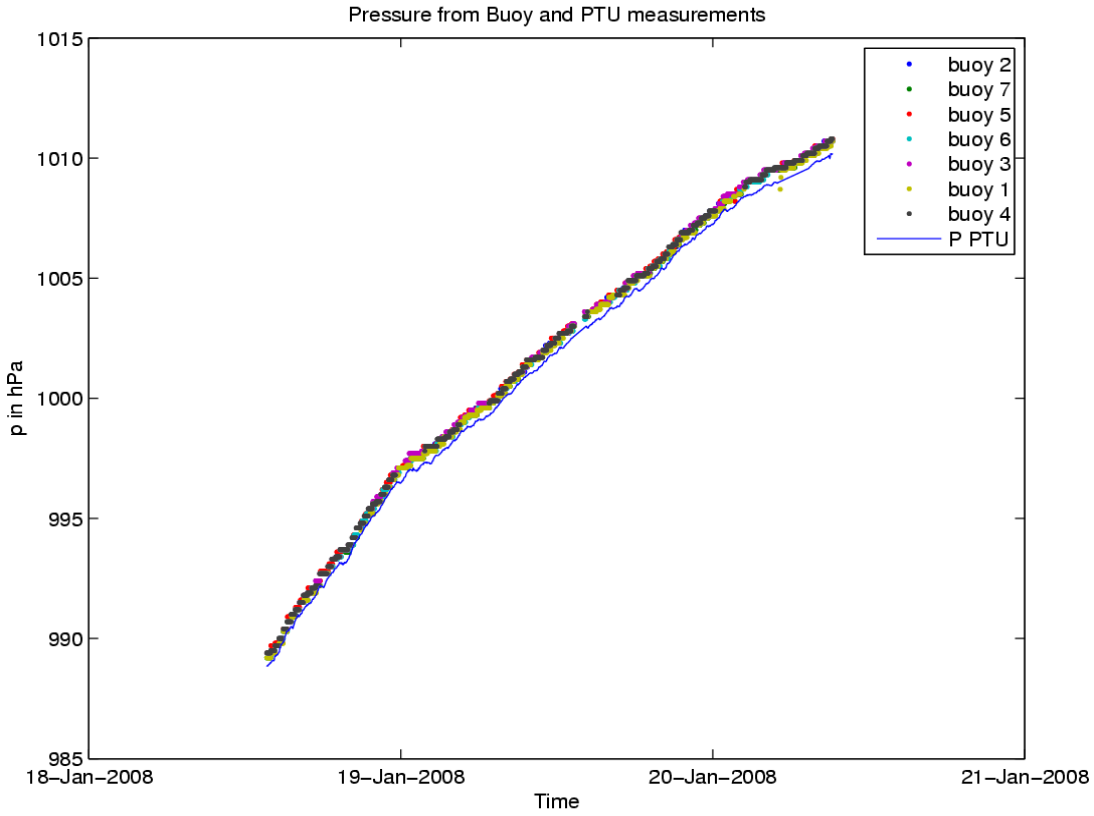

Fig. 2.1: Pressure calibration measurement in the hangar at Longyearbyen airport of all 7 buoys (points) and the PTU reference unit (line) from 18 January 12:26 LT to 20 January, 9:05 LT.

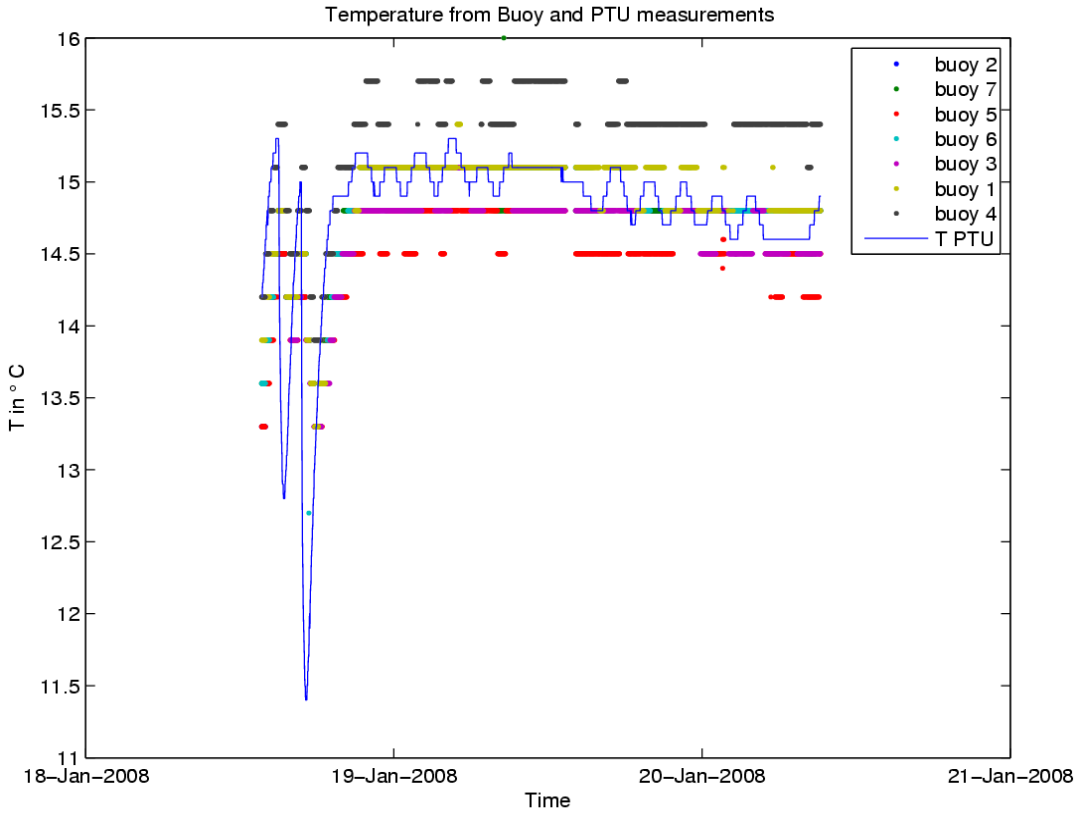

Fig. 2.2: Temperature calibration measurements in the hangar at Longyearbyen airport of all 7 buoys (points) and the PTU reference unit (line) from 18 January 12:26 LT to 20 January, 9:05 LT.

2.3 Buoy drop mission

The seven CALIB ice buoys were launched on the ice in the northern entrance of the Fram Strait between 82°N – 83°N and 5°W – 15°E on late 20 January 2008. The parachute-equipped buoys were dropped on ice from a DO-228 aircraft of the Norwegian company Lufttransport, which operated from the airfield in Longyearbyen on Spitsbergen (Figure 2.3). The deployment/initial positions of the 7 buoys are depicted in Figure 3.1.

From preceding drop missions in connection with earlier FRAMZY campaigns it became clear, that visual assessment of the in-situ ice conditions around the planned drop positions by the pilots is very important for a “last-minute-fine-adjustment” of the drop positions in order to avoid dropping the buoys on thin or broken ice or even into open water. Hence, dropping buoys on ice at such high latitudes as early in the year as in case of FRAMZY 2008 is difficult, because no daylight is available due to prevailing polar night. For that reason the day of the mission was chosen close to the date of full moon (22 January 2008). During the flight mission it showed up, that moon light was sufficient to make ice conditions visible enabling the pilots to find places suited for dropping the buoys. All 7 buoys were dropped over relatively closed ice and no buoy was lost after the drop.

Fig. 2.3: **Above:** Looking for the right ice conditions for the “fine adjustment” of location for buoy-deployment. **Below:** CALIB buoy just after dropping with parachute shortly before opening. These photos are taken during a buoy-drop mission very similar to that of FRAMZY 2008, but performed (under daylight conditions) about one year before in March during FRAMZY 2007.

3. Summary of buoy measurements and synoptic conditions

This section gives a summary of the buoy measurements, and it describes briefly the synoptic conditions encountered in the Fram Strait region during the experiment.

3.1 Measurements of the seven ARGOS ice buoys

Figure 3.1 shows the trajectories of all 7 ice buoys from 20 January until 28 February 2008. The lifetime of the buoys differed from four days for buoy B4 to 40 days for buoy B1, B2 and B5. Only one buoy (B6) reached the ice edge and got lost there. All other buoys were lost in the pack ice.

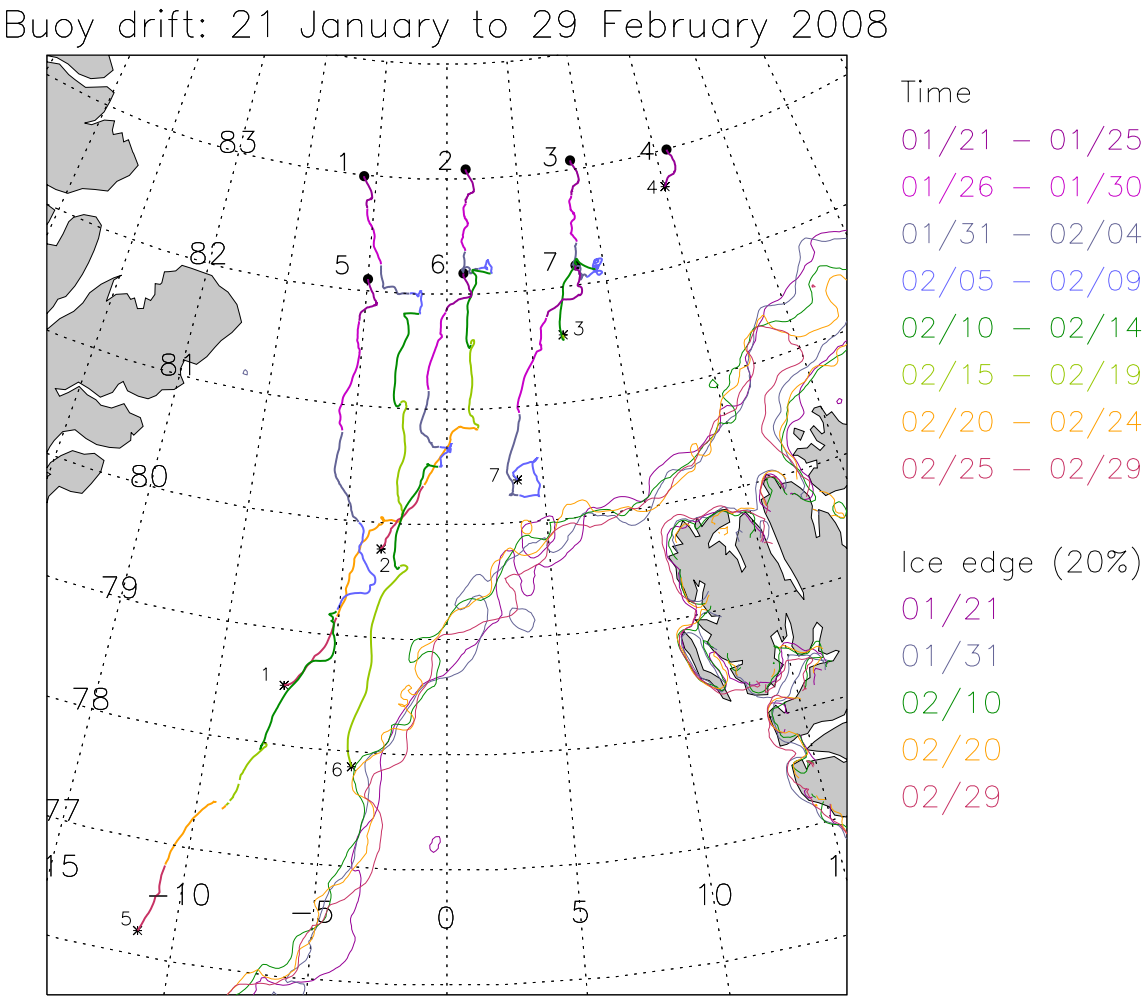

Fig. 3.1: Start positions (black dots), trajectories and end positions (stars) of the seven ice buoys (labeled 1-7). Different colors hold for time intervals of 5 days each. Thin lines mark the ice edge taken from AMSR-E satellite data (see Appendix A2).

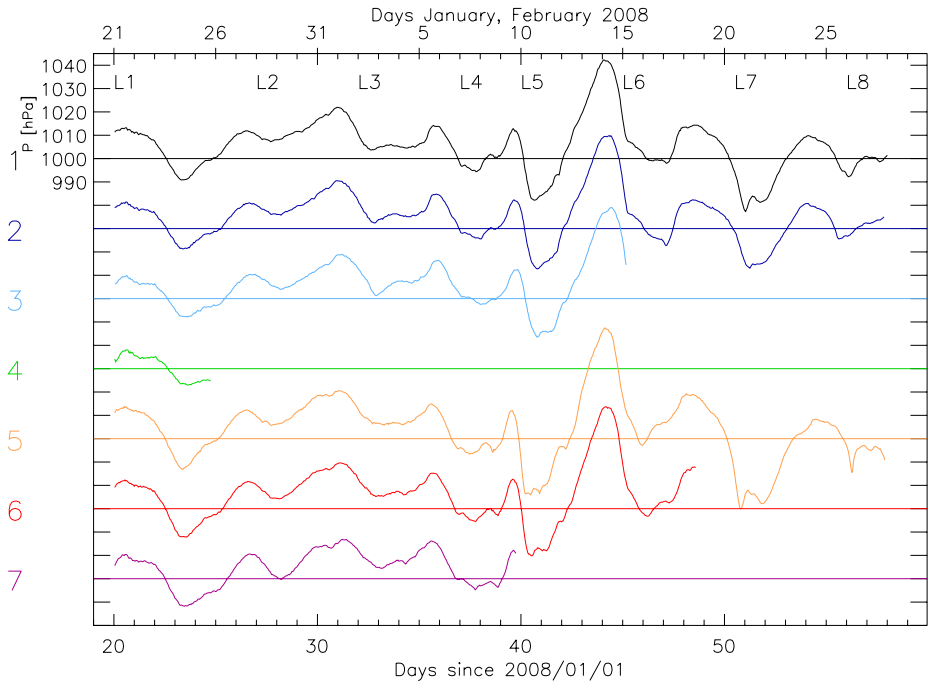

Fig. 3.2: Pressure time series of all seven ice buoys. Horizontal lines mark respective 1000 hPa value. L1-L8 mark eight cyclone events

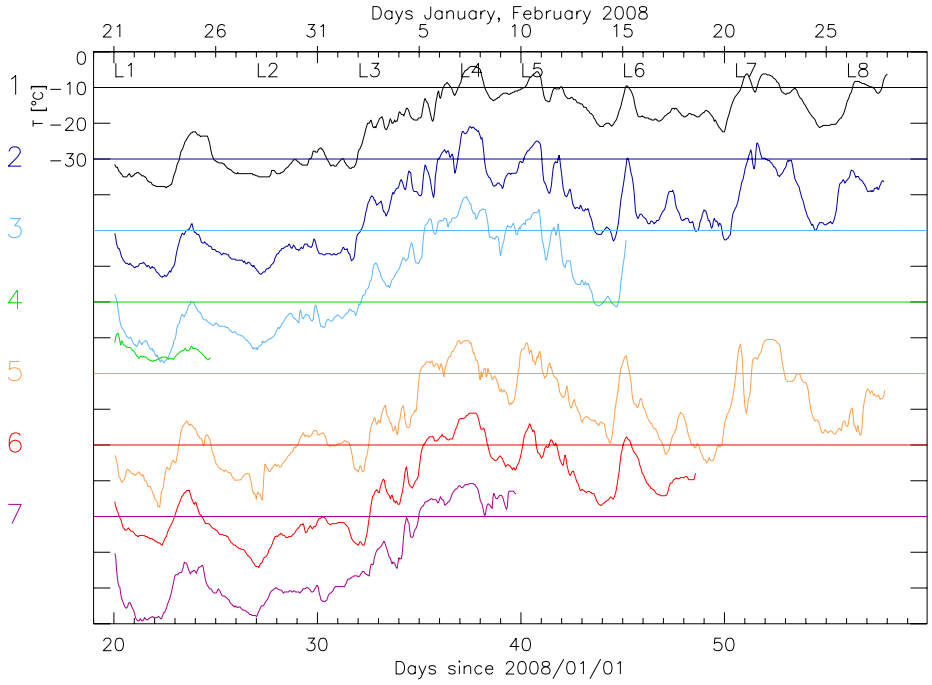

Fig. 3.3: Temperature time series of all seven ice buoys. Horizontal lines mark respective -10° C value. L1-L8 mark eight cyclone events.

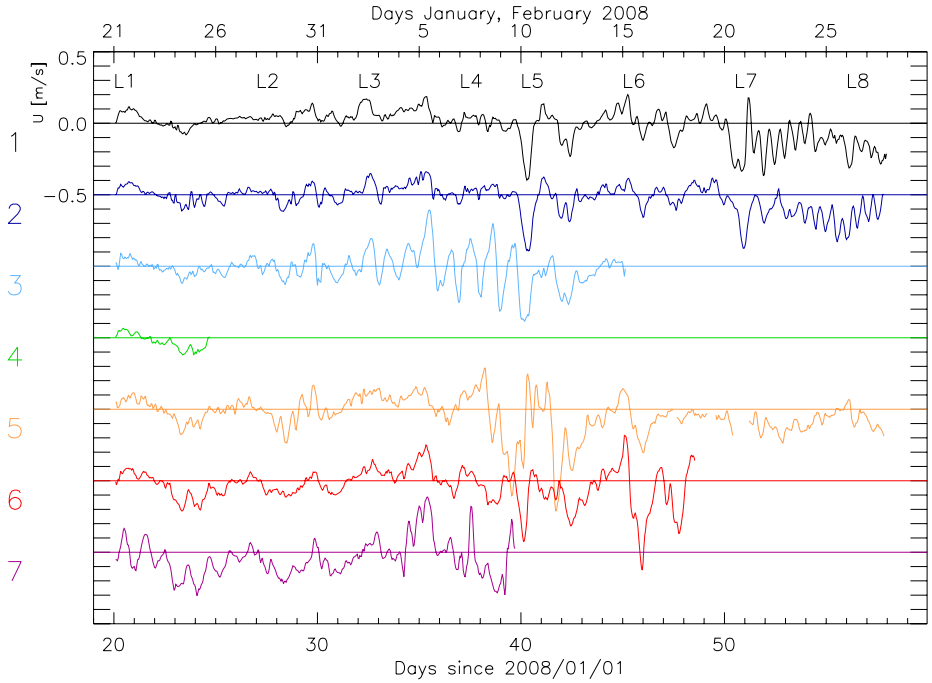

Fig. 3.4: West-east drift component (u) time series of all seven ice buoys. Horizontal lines mark respective 0 m/s value. L1-L8 mark eight cyclone events.

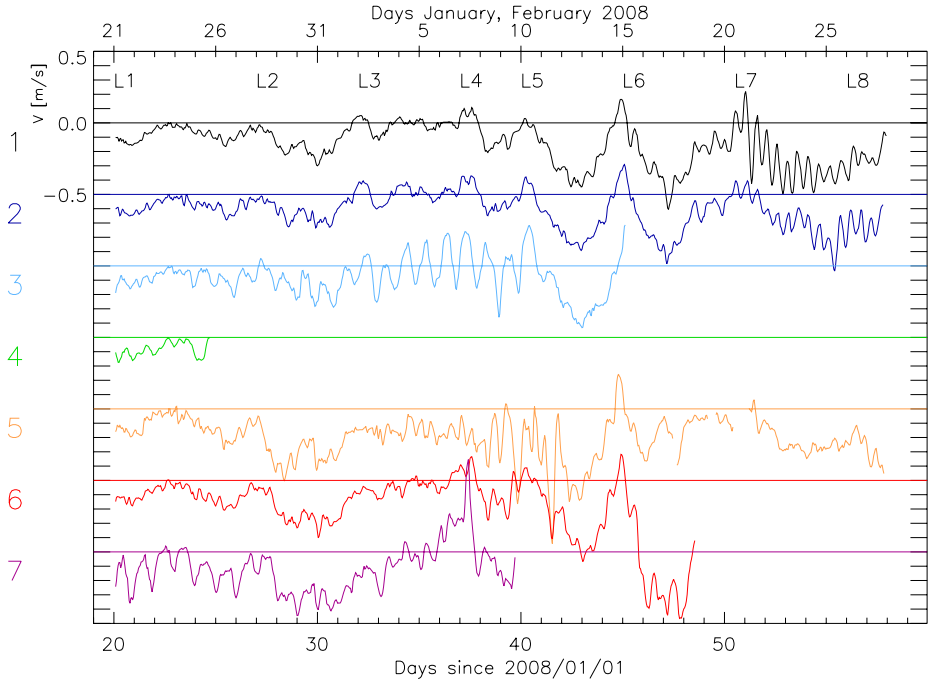

Fig. 3.5: South-north drift component (v) time series of all seven ice buoys. Horizontal lines mark respective 0 m/s value. L1-L8 mark eight cyclone events.

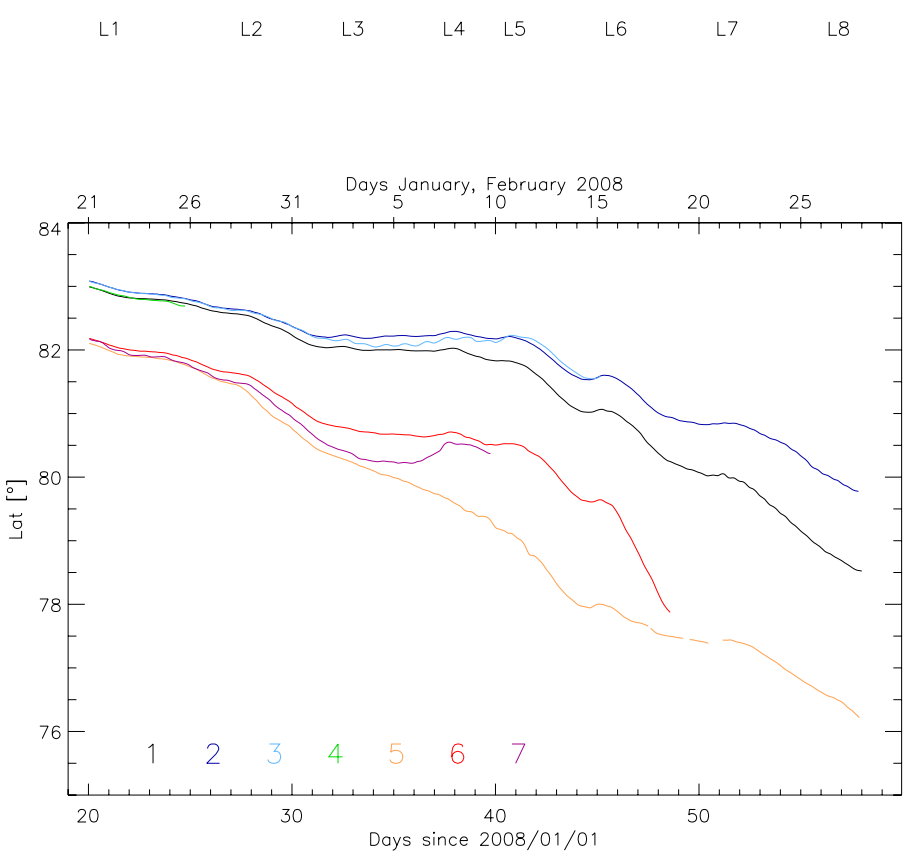

Fig. 3.6: Time series of latitude of all seven ice buoys.

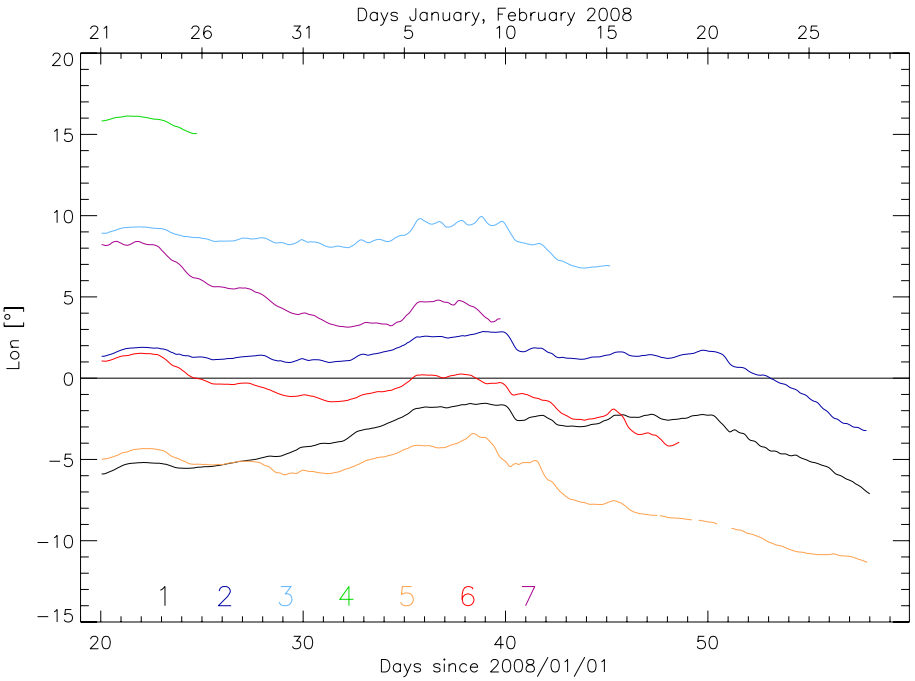

Fig. 3.7: Time series of longitude of all seven ice buoys.

Figures 3.2 and 3.3 display the time series of pressure and temperature. Air pressure varied between 970 and 1045 hPa. The synoptic-scale features are reflected similarly in all buoy pressure time series. Eight low-pressure events affected the Fram Strait during the experimental period. They are marked by L1-L8 in the figures and in the sea-level pressure maps in Appendix A1. The temperature varied between -40° C and 0° C. Again, the synoptic-scale temperature variations are similarly reflected at all buoys. At the beginning of February temperatures rose by 15-20 K and remained at a higher level until the end of the experiment.

The drift velocity is presented for the east-west (u) and north-south (v) component in Figures 3.4 and 3.5, respectively. The temporal resolution of the measured ice drift is 1 hour. The u component varied between -0.6 and 0.4 ms^{-1} and the v component between -0.9 and 0.6 ms^{-1}. The mean values (averaged over all buoys and data) amount to -0.03 ms^{-1} for the u component and -0.15 ms^{-1} for the v component of ice drift. The strongest positive values of the v component (northward ice drift) always occurred in relation to cyclone passages. Buoy B3 shows a strong diurnal oscillation in both components from 31 January to 11 February. Buoys B1 and B2 encounter a semidiurnal oscillation starting on 21 February.

Figures 3.6 and 3.7 show the time series of latitude and longitude positions of all buoys. Until 1 February the buoys drifted southward with moderate speed. From 1 to 9 February almost all buoys remained at nearly constant latitude. After 9 February the buoys drifted again southward, but now with higher speed.

The hourly positions of the ice buoys are used to calculate the ice drift divergence four selected buoy triangles (T1 to T4). Figure 3.8 shows their locations every 2 days. After deployment all triangles had nearly the same size. Due to different buoy drift velocities the triangles deformed in the course of the time. The time series of ice drift divergence for the four triangles and for the total area are presented in Figure 3.9 for the period from 21 January to 07 February as long as all six buoys were working. During the first days all triangles, except T4, showed a similar divergence. The divergence of T4 had a higher degree of variability due to the high north-south drift fluctuations of buoy B7 which was nearest to the ice edge. Divergence fluctuations of all triangles increased with time. The total area of all four triangles showed smaller divergence fluctuations than the individual triangles.

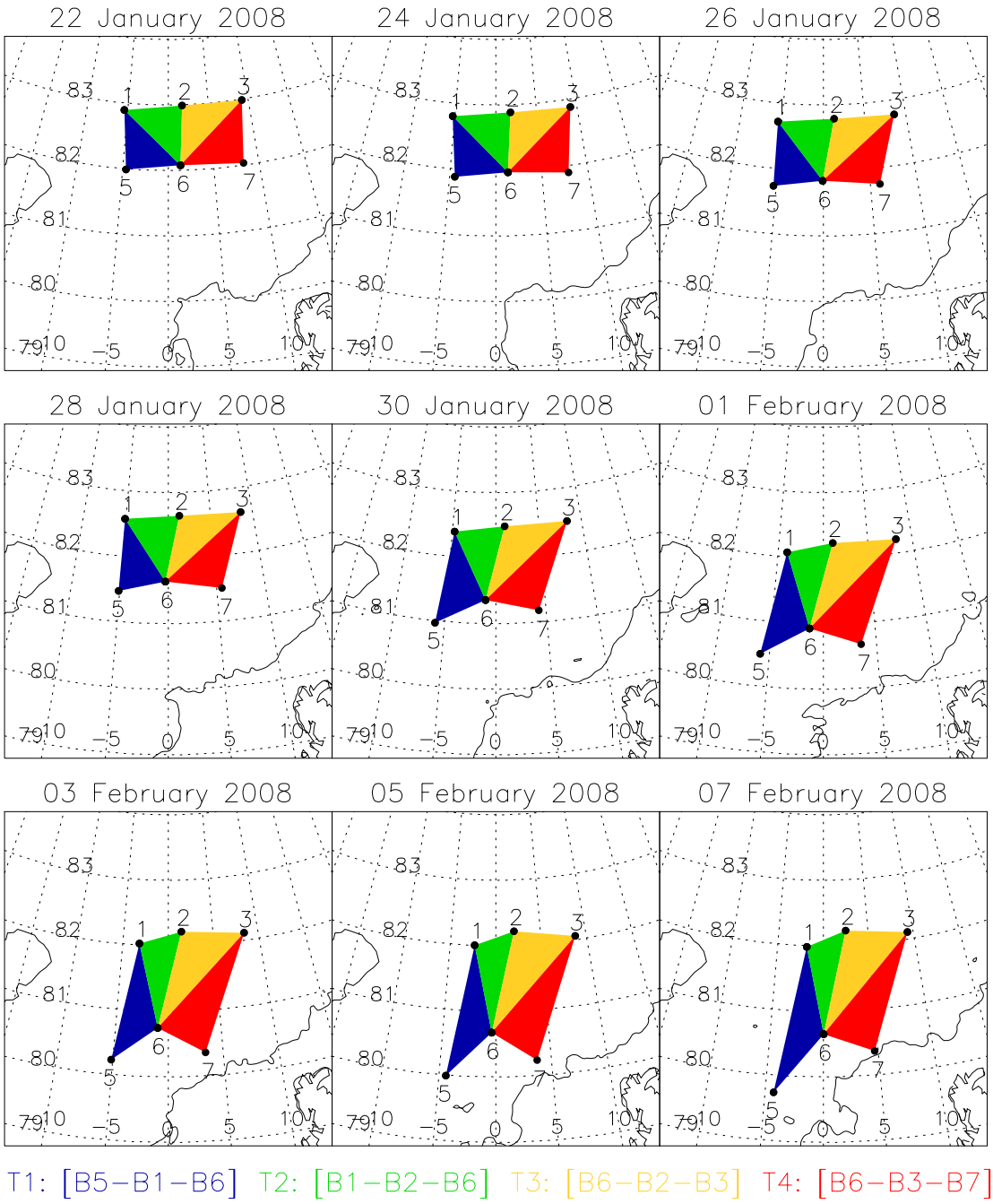

Fig. 3.8: Buoy triangles T1-T4 every 2 days between on 22 January and 7 February 2008.

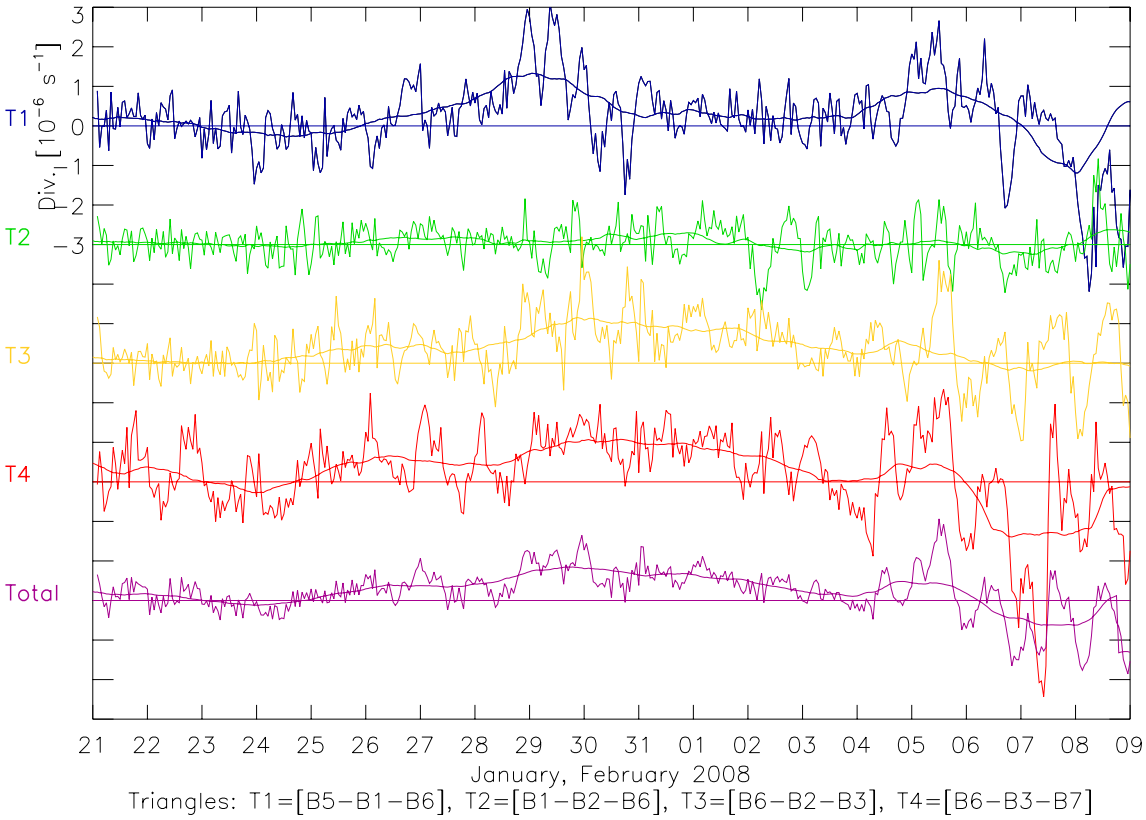

Fig. 3.9: Time series of ice drift divergence for buoy triangles T1-T4 (see Figure 3.8) and for the total area of all four triangles for 21 January to 07 February. Horizontal lines mark respective 0 s^{-1} value.

The hourly buoy positions are used to calculate the length of the drift trajectory for each buoy for a time interval of 512 hours starting on from 21 January. Additionally, the lengths of the trajectories for lower temporal resolutions are calculated. Figure 3.10 displays the length depending on the time resolution, normalized with the length based on the highest one hour resolution. Figure 3.10 shows substantial differences in relative drift length for the individual buoys. The relative drift length varies (for the 512 hours = 21,3 days) between 0.85 (buoy B5) and 0.35 (buoy B3). Under the assumption that the atmospheric forcing was the same for each buoy, these ratios are indications of different ice conditions (ice compactness) in which the drifting buoys were embedded.

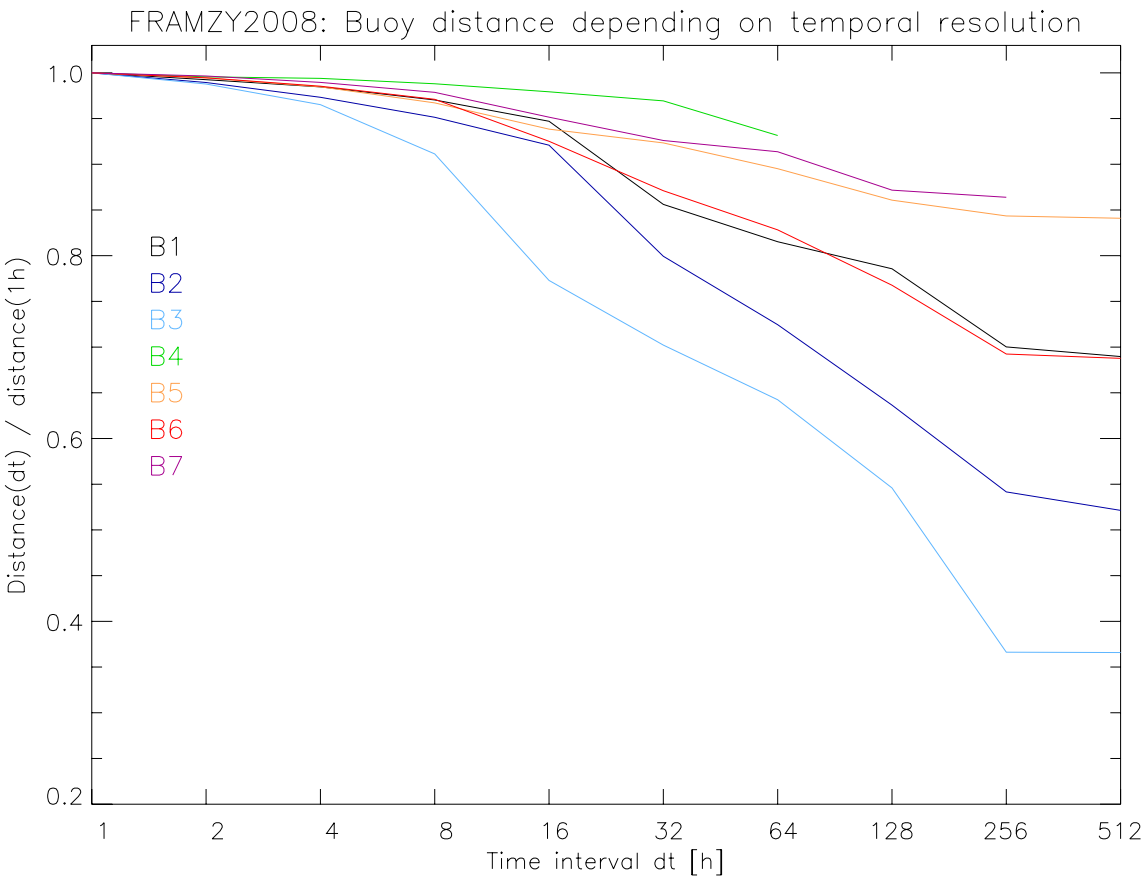

Fig. 3.10: Length of drift trajectory for each buoy for a time period of 512 hours but measured with different time resolution between 1 and 512 hours. The length of the trajectory is normalized with the length calculated with the highest (1 hour) time resolution.

3.2 Summary of synoptic conditions in Fram Strait region

The synoptic conditions in the Fram Strait region during the FRAMZY 2008 buoy experiment from 20 January to 28 February 2008 are represented in Appendix A1 by 12-hourly maps of sea-level pressure and 2 m air temperature as analysed by the European Centre for Medium Range Weather Forecasts (ECMWF). A start description of the synoptic conditions is listed in Table 3.1. During FRAMZY 2008 8 cyclones passed through Fram Strait and affected the sea ice. The cyclones are labeled L1 to L8 and the times of there occurrences are marked in the buoy data time series in Figs. 3.2 to 3.5. Except for the loss of buoy B7, all other buoy losses were connected with the impact of a cyclone. The last three buoys, B1, B2, B5, were lost simultaneously in the night from 27 to 28 February 2008, when every strong cyclone event L8 occurred. Interestingly, the three buoys were about 200 km apart from each other and were not located close to the ice edge (still about 50 km away) at the time of loss.

Table 3.1: Presence of buoys B1-B7 (a lost buoy is marked by -) and brief description of synoptic condition between 20 January and 28 February 2008.

Month	Day	Buoys present	Synoptic Situation
1	20	1 2 3 4 5 6 7	Deployment of all 7 buoys during full moon. High over Greenland. Weak high pressure ridge over Fram Strait. W wind over buoy array.
1	21	1 2 3 4 5 6 7	Weak cyclone L1 develops at NE coast of Greenland. L1 moves E over buoy array. First weak wind, later strong NW wind on rear side of cyclone L1.
1	22	1 2 3 4 5 6 7	Cyclone L1 moves E-wards and leaves Fram Strait. First strong NW wind. Later weak N/NW wind under weak anticyclonic influence coming from W.
1	23	1 2 3 4 5 6 7	E wind between weak high pressure bridge in the N and decreasing low pressure over Greenland Sea with trough T1 extending into eastern part of Fram Strait.
1	24	1 2 3 4 5 6 7	Moderate to strong N/NE wind between ridge in the N extending from Northern Greenland NE-wards and cyclone pair S of Fram Strait and Spitsbergen.
1	25	1 2 3 - 5 6 7	Strong N wind between high over Greenland and ridge extending NE-wards and cyclone moving from SW to E/NE over Svalbard.
1	26	1 2 3 - 5 6 7	Strong N wind between weak high pressure zone N of Greenland and cyclone over Barents Sea.
1	27	1 2 3 - 5 6 7	Decreasing N wind. Later weak N/NW wind in high pressure ridge extending from N-Greenland into N-part of Fram Strait.
1	28	1 2 3 - 5 6 7	N part of Fram Strait under high pressure ridge with weak NE wind. S part of Fram Strait under influence of cyclone SW of Svalbard with strong NE wind.
1	29	1 2 3 - 5 6 7	N wind in Fram Strait. Weak in N part, strong in S part. High over Greenland. Low over northern Barents Sea. Weak low L2 (cold core low at 500 hPa) approaches from NW over the Arctic Ocean.
1	30	1 2 3 - 5 6 7	N wind in Fram Strait. As on day before: weak in N part, strong in S part. L2 moves from N to S through Fram Strait, but has almost no signatures at the surface.
1	31	1 2 3 - 5 6 7	L2 (at 500 hPa level) now S of Fram Strait. Fram Strait in moderate (in the N part) to strong N/NE wind.
2	1	1 2 3 - 5 6 7	High pressure ridge propagates from W into Fram Strait. N wind decreases, later variable wind.
2	2	1 2 3 - 5 6 7	High pressure ridge moves further E/SE. Weak cyclone L3a moves in from W, but influences only N part of Fram Strait.

Month	Day	Buoys present	Synoptic Situation
2	3	1 2 3 - 5 6 7	Weak wind: first variable, later from S/SW. Weak high pressure over Svalbard and low L3b N of Greenland.
2	4	1 2 3 - 5 6 7	S/SW wind in Fram Strait: weak to moderate. High SE of Svalbard. Low L3b N of Greenland.
2	5	1 2 3 - 5 6 7	S wind, later SE/E wind: moderate to weak. High over northern Barents Sea with ridge extending to area N of Fram Strait.
2	6	1 2 3 - 5 6 7	High pressure ridge moves N-ward. Low pressure system L4 developes along E coast of Greenland. Wind turns from E to S/SE and increases.
2	7	1 2 3 - 5 6 7	Low pressure system L4 with several cores extends from S to N in western part of Fram Strait over sea ice. First strong, later decreasing S wind in Fram Strait.
2	8	1 2 3 - 5 6 7	Low pressure system L4 effects still Fram Strait. It moves NE-ward. Winds in Fram Strait variable (in direction and strength) depending on relative location to cyclone core.
2	9	1 2 3 - 5 6 7	L4 system leaves Fram Strait towards NE. Weak high pressure ridge follows in northern Fram Strait. New strong cyclone L5 approaches from SW along E coast of Greenland. Wind weak and later from E.
2	10	1 2 3 - 5 6 7	Strong cyclone L5 (~ 975 hPa) moves from SW to NE towards Fram Strait, but still with its core S of 78° N. First strong E/NE wind, later weaker E/SE wind.
2	11	1 2 3 - 5 6 -	Cyclone L5 and a long southward extending trough propagate from SW to NE through Fram Strait. Later strong N wind field approaches from N.
2	12	1 2 3 - 5 6 -	Strong N wind on rear side of cyclone L5 which deepened to 965 hPa and is now over Novaja Semlja.
2	13	1 2 3 - 5 6 -	Strong N wind, later decreasing and backing to NW with an approaching high pressure zone from W.
2	14	1 2 3 - 5 6 -	High pressure zone moves from W to E over Fram Strait in the course of the day. Wind changes from NW to S. A new cyclone L6 is present at the N coast of Greenland with a trough extending along the E coast of Greenland.
2	15	1 2 - - 5 6 -	Cyclone L6 developes at NE coast of Greenland and moves E/SE. Wind first strong from S ahead of cyclone, later strong from N behind cyclone L6.
2	16	1 2 - - 5 6 -	Cyclone L6 moves over Svalbard towards E. Fram Strait in strong NE, later NW wind. Weak upper level cold core N of Greenland is included into the upper level cyclonic circulation of L6.

Month	Day	Buoys present	Synoptic Situation
2	17	1 2 - - 5 6 -	Nearly unchanged situation. Strong N/NW wind in Fram Strait between cyclone L6 E of Svalbard and high pressure over NE-Greenland.
2	18	1 2 - - 5 - -	NW/W wind over Fram Strait weakening in the course of the day. Cyclone L6 E of Svalbard and high over NE-Greenland still present, but much weaker.
2	19	1 2 - - 5 - -	High pressure zone approaches from W and lies over Fram Strait in the course of the day. Weak variable wind.
2	20	1 2 - - 5 - -	High pressure zones moves further NE. Low pressure system L7 developes and deepens (< 970 hPa) at E coast of Greenland. Increasing SE/E wind in Fram Strait.
2	21	1 2 - - 5 - -	Cyclone L7 weakens and degenerates to a trough and is incorporated into the circulation system of a very strong (< 950 hPa) cyclone near Jan Mayen. E wind in E part, N wind in W part of Fram Strait.
2	22	1 2 - - 5 - -	Cyclonic influence retreats towards S. High pressure influence approaches from N. Wind from E to N in Fram Strait.
2	23	1 2 - - 5 - -	Strong N/NE wind. High pressure N of Greenland. Low pressure over Norwegian Sea.
2	24	1 2 - - 5 - -	Strong N/NE wind. High pressure over Greenland. Low pressure near Lofotes Islands. Upper level cold core moves southward over Svalbard and eastern part of Fram Strait.
2	25	1 2 - - 5 - -	Upper level cold core leads to strong cyclone L8 development over the open water W of Svalbard. Strong NE/N wind is over the ice-covered part of Fram Strait.
2	26	1 2 - - 5 - -	Cyclone L8 moves along an unusual track from NE to SW along the Fram Strait ice edge and weakes at the surface, but remains at upper levels. Strong N/NE wind over ice-covered part of Fram Strait.
2	27	1 2 - - 5 - -	An intense surface low L8 developes (< 985 hPa) on the N side of the upper level cold core low. Very strong winds on the west side of L8.
2	28	1 2 - - 5 - -	The intense low L8 has a very short life time and nearly dissolved in the course of the day. NE wind over the ice. The last three buoys are lost in the night from 27 to 28 February when L8 was most intense.

4. Examples of measurements

Three examples of the atmospheric forcing of the sea ice drift in the Fram Strait are detailed below. These examples are:

(1) a period of strong off-ice air flow,

(2) the passage of a cyclone (L4) through Fram Strait,

(3) the atmospheric conditions before the simultaneous loss of three ice buoys.

4.1 Strong off-ice air flow over Fram Strait

Off-ice air flow over the entire Fram Strait occurs when the dominating pressure centers are rather far away, i.e. when the high pressure center is located over Greenland and low pressure is situated over the Greenland Sea or Barents Sea. Such a synoptic situation was present on 29 and 30 January 2008 (see Appendix A1). At this time the buoy array was centered around 82° N, 0° E and was in the region of pack ice with high ice concentration. Air temperatures were around -30° C. The off-ice air flow caused an acceleration of the southward ice drift to -0.45 ms^{-1}, a value which was about twice as large as the average value during the 7 days before (Figure 3.5). Since the pressure gradient was stronger in the southern part of the buoy field, the southerly ice drift was stronger there than in the northern part. At this time, the buoy array encountered increased ice drift divergence (Figure 3.9).

4.2 Passage of cyclone L4 through Fram Strait

The passage of cyclone L4 through Fram Strait occurred on 7 and 8 February 2008. The cyclone developed between Iceland and Jan Mayen on 6 February and moved northeastward. Its track was situated between the ice edge and the east coast of Greenland and later further north over the pack ice where it weakened. The temporal changes of sea level pressure, temperature and ice drift in the buoy array during the period 7-8 February are presented in Fig. 4.1. Ahead of L4 warm air was transported from S/SE into the buoy array causing a temperature increase of 7-10 K. The general southward ice drift in Fram Strait ceased and for almost one day even a northward ice drift was measured in the buoy array. After the passage of L4 the air temperature dropped by 15 K when the wind turned to northerly direction. The ice drift returned to the normal direction. This sequence of temperature and ice drift variations is typical for cyclones whose south-north track is situated in the western part of the Fram Strait. The passages of L5, L6 and L7 show a similar sequence of events (see Figures 3.2-3.5) and even with a larger amplitude than cyclone L4. Cyclone L4 was selected for demonstration here, because still six buoys were operating and, thus, the data coverage was better than for the other cyclone events.

Fig. 4.1 shows that the drift buoy 35 deviated substantially from the drift of the other buoys. Its drift direction was even opposite to the geostrophic wind forcing. The reason for the stronger behaviour of B5 is yet unknown. An error in the drift determination can be excluded. Also a comparison of the buoy pressure measurements with the ECMWF sea-level pressure analysis shows no major discrepancies. Thus, it must be concluded that there was a strong oceanic forcing at B5.

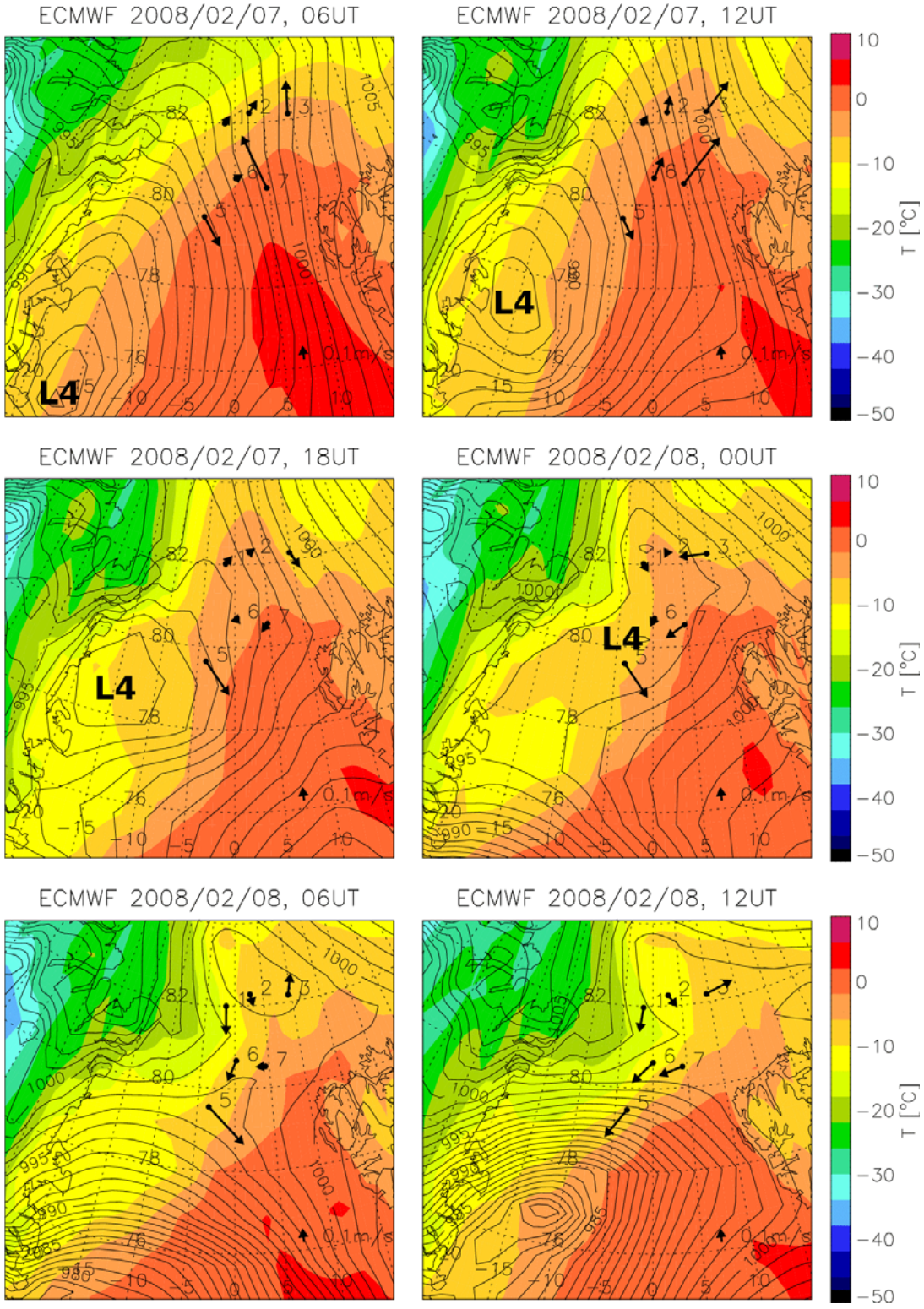

Fig. 4.1: Six-hourly maps of sea-level pressure and temperature from ECMWF analyses and ice drift from CALIB buoys during the passage of cyclone L4 on 7-8 February 2008.

4.3 The simultaneous loss of three ice buoys – possible reasons

Three ice buoys (B1, B2, B5) were lost almost at the same time in the night from 27 to 28 February 2008. It was the loss of the last buoys and, thus, terminated the FRAMZY 2008 ice drift experiment. At the time of loss the buoys were still about 50 km away from the ice edge and were distributed almost along a straight line between 76 and 80° N (Figure 3.1). The synoptic situation during the days before the loss is illustrated in Appendix A1. On 24 February 2008 a low pressure system developed north of Jan Mayen and moved very slowly northeastward on 25 and 26 February. The cyclone track passed south of Svalbard. A trough with an embedded cyclone L8 developed over the open water on the westside of Svalbard. Trough and cyclone propagated southwestwards (a very seldom propagation direction) and overrun the 3 ice buoys. Behind trough and cyclone strong easterly on-ice airflow occurred for almost 2 days over the western ice-covered part of the Fram Strait where the last three buoys were situated. The long fetch of the wind over open water presumably caused high waves and, thus, high swell in the ice near the ice edge. In this situation the buoys got lost. It may be presumed that the sea ice (even at places of 50 km distance from the ice edge) broke at many places in the area and that the ice got flooded from below through the leads. The CALIB buoys are lying flat on the snow/ice surface after landing with the parachute and they are not particularly protected against water. As soon as water enters into the buoy's electronics, the operation stops.

5. Conclusions

FRAMZY 2008 was the fourth and smallest of the FRAMZY experiments focussing on Fram Strait cyclones and their impact on sea ice. Concerning the number of experimental platforms only seven CALIB buoys were employed. During the five weeks experimental period eight cyclones passed through Fram Strait, more than during the preceding experiments. Depending on the location of the track, the cyclones caused variations of the Fram Strait ice export which reached from stagnation or even reversal to strong acceleration. With the FRAMZY 2008 measurement took place for the first time in mid-winter (January and February). The data set of all FRAMZY experiments now covers the full range of wintertime synoptic conditions and sea ice drift in Fram Strait from mid-January to the end of April.

Acknowledgement

The buoy drift experiment was funded by the German Science Foundation (DFG) under the grant SFB 512 "Cyclones and the North Atlantic climate system". We thank our colleague, Werner Biselli, who was responsible for the technical preparation and deployment of the CALIB buoys from the DO-228 aircraft.

Literature

Affeld, B., 2003: Zyklonen in der Arktis und ihre Bedeutung für den Eistransport durch die Framstraße. Ph.D. Thesis, University of Hamburg, 130 pp.

Brümmer, B. (Ed.), 2000: Field experiment FRAMZY 1999: Cyclones over the Fram Strait and their impact on sea ice – Field report with examples of measurements. Ber. a.d. Zentrum f. Meeres- und Klimaforschung, Reihe A, Meteorologie, Nr. 33, 176 pp.

Brümmer, B. and H. Hoeber, 1999: A mesoscale cyclone over the Fram Strait and its effects on sea ice. J. Geophys. Res., 104, 19.085-19.098.

Brümmer, B., G. Müller and H. Hoeber, 2003: A Fram Strait cyclone: properties and impact on ice drift as measured by aircraft and buoys. J. Geophys. Res., 108, 4217, doi: 10.1029/2002JD002638.

Brümmer, B., G. Müller and D. Schröder, 2005: In situ observations in cyclones over Fram Strait. Meteorol. Zeitschrift, Vol. 14, No. 5, 721-734.

Brümmer, B., J. Launiainen, G. Müller and D. Schröder, 2005: FRAMZY 2002: Second field experiment on Fram Strait cyclones and their impact on sea ice. Ber. a.d. Zentrum f. Meeres- u. Klimaforschung, Reihe A, Meteorologie, Nr. 37, 154 pp.

Brümmer, B, G. Müller, A. Lammert and A. Jahnke-Bornemann, 2009: FRAMZY 2007: Third field experiment on Fram Strait cyclones and their impact on sea ice. Ber. a.d. Zentrum f. Meeres- und Klimaforschung, Reihe A, Meteorologie, in preparation.

Jahnke-Bornemann, A. and B. Brümmer, 2008: The Iceland-Lofotes pressure difference seesaw with the North Atlantic low pressure zone. Submitted to Tellus A.

Kauker, F., A. Gerdes, M. Karcher, C. Köberle and J.L. Lieser, 2003: Variability of Arctic and North Atlantic sea ice. J. Geophys. Res., 108 (C6), 3182, doi: 10.1029/2002JC001573.

Kriegsmann, A. and B. Brümmer, 2008: Sensitivity studies of cyclone impact on sea ice in a coupled ice-ocean model. Submitted to Geophys. Res. Letters.

Kwok, R., G.F. Cuningham and S.S. Pang, 2004: Fram Strait sea ice outflow. J.Geophys. Res., 109 (C1), C 01009, doi: 10.1029/2003JC001785.

Lammert, A. and B. Brümmer, 2008: Observation of cyclone – induced inertial sea ice oscillation in Fram Strait. In preparation.

Rasmussen, E.A., P. Guest and K. Davidson, 1997: Synoptic and mesoscale features over the ice-covered portion of the Fram Strait in spring. J. Geophys. Res., 102, 13.975-13.986.

Schröder, D., 2005: Wirkung von Zyklonen auf das Meereis in der Framstraße: Modellrechnungen und Beobachtungen. Ph.D. Thesis, University of Hamburg, 135 pp.

Spreen, G., 2008: Satellite-based estimates of sea-ice volume flux: applications to the Fram Strait region. Ph.D. Thesis, University of Hamburg, 172 pp.

Spreen, G., L. Kaleschke and G. Heygster, 2008: Sea ice remote sensing using AMSR-E 89 GHz channels. J. Geophys. Res., doi: 10.1029/2005JC003384.

Vinje, T., 2001: Fram Strait ice fluxes and atmospheric circulation: 1950-2000. J. Climate, 14 (6), 3508-3517.

Vinje, T., N. Nordlund and A. Kambekk, 1998: Monitoring ice thickness in Fram Strait. J. Geophys. Res., 103 (C5), 10437-10449.

Appendix

A1 ECMWF surface analyses

Appendix A1 lists 12-hourly maps of sea-level pressure and 2 m temperature as analysed by the European Centre for Marine-Range Weather Forecasts (ECMWF). The actual positions of the CALIB ice buoys are marked by black dots. H. L mark highs and lows. L1-L8 mark lows which are referred to in the text.

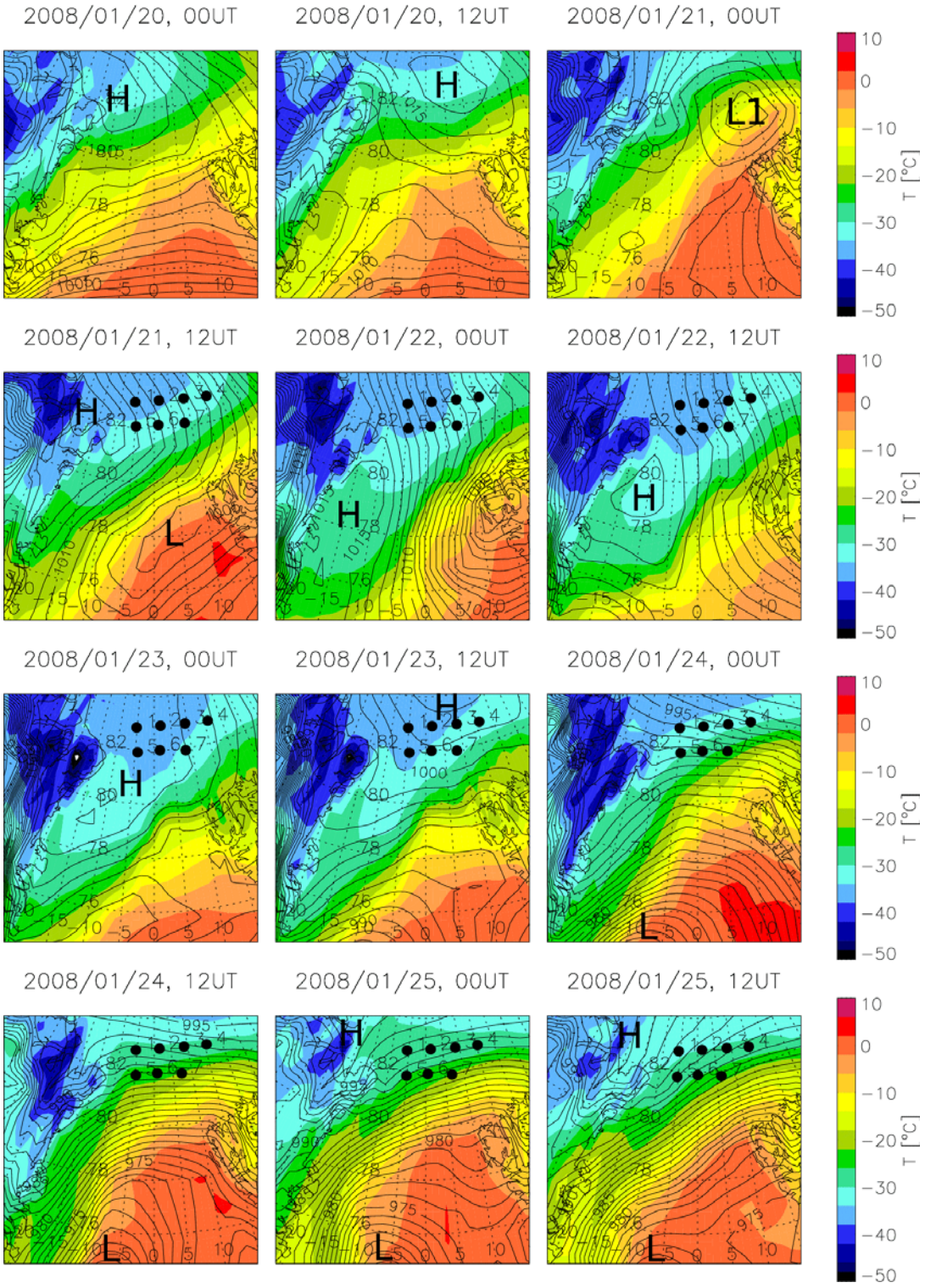

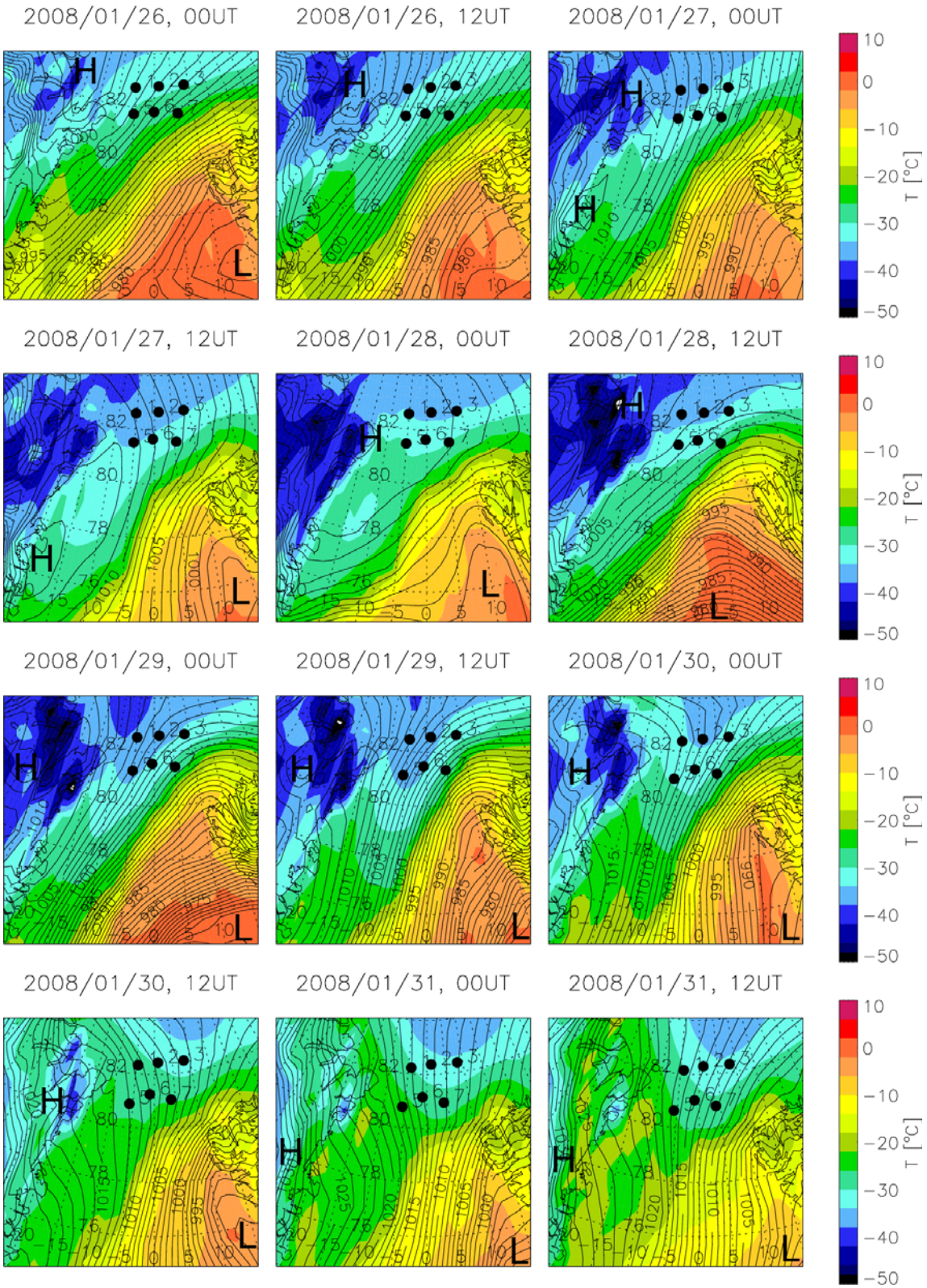
2008/01/26, 00UT
2008/01/26, 12UT
2008/01/27, 00UT
2008/01/27, 12UT
2008/01/28, 00UT
2008/01/28, 12UT
2008/01/29, 00UT
2008/01/29, 12UT
2008/01/30, 00UT
2008/01/30, 12UT
2008/01/31, 00UT
2008/01/31, 12UT
T [°C]
10
0
−10
−20
−30
−40
−50

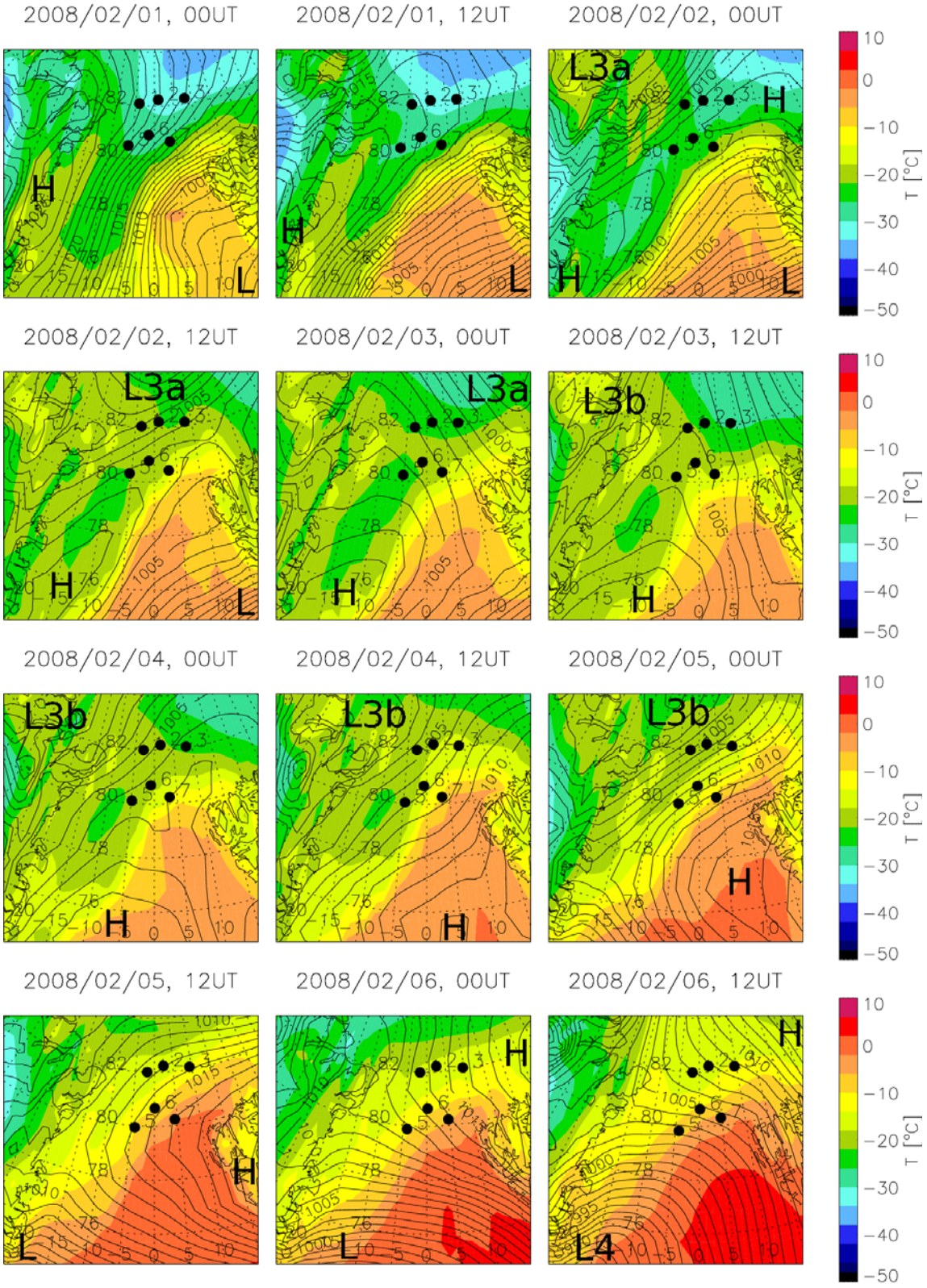
2008/02/01, 00UT
2008/02/01, 12UT
2008/02/02, 00UT
2008/02/02, 12UT
2008/02/03, 00UT
2008/02/03, 12UT
2008/02/04, 00UT
2008/02/04, 12UT
2008/02/05, 00UT
2008/02/05, 12UT
2008/02/06, 00UT
2008/02/06, 12UT
L3a
L3b
L4
H
L
T [°C]
10
0
−10
−20
−30
−40
−50

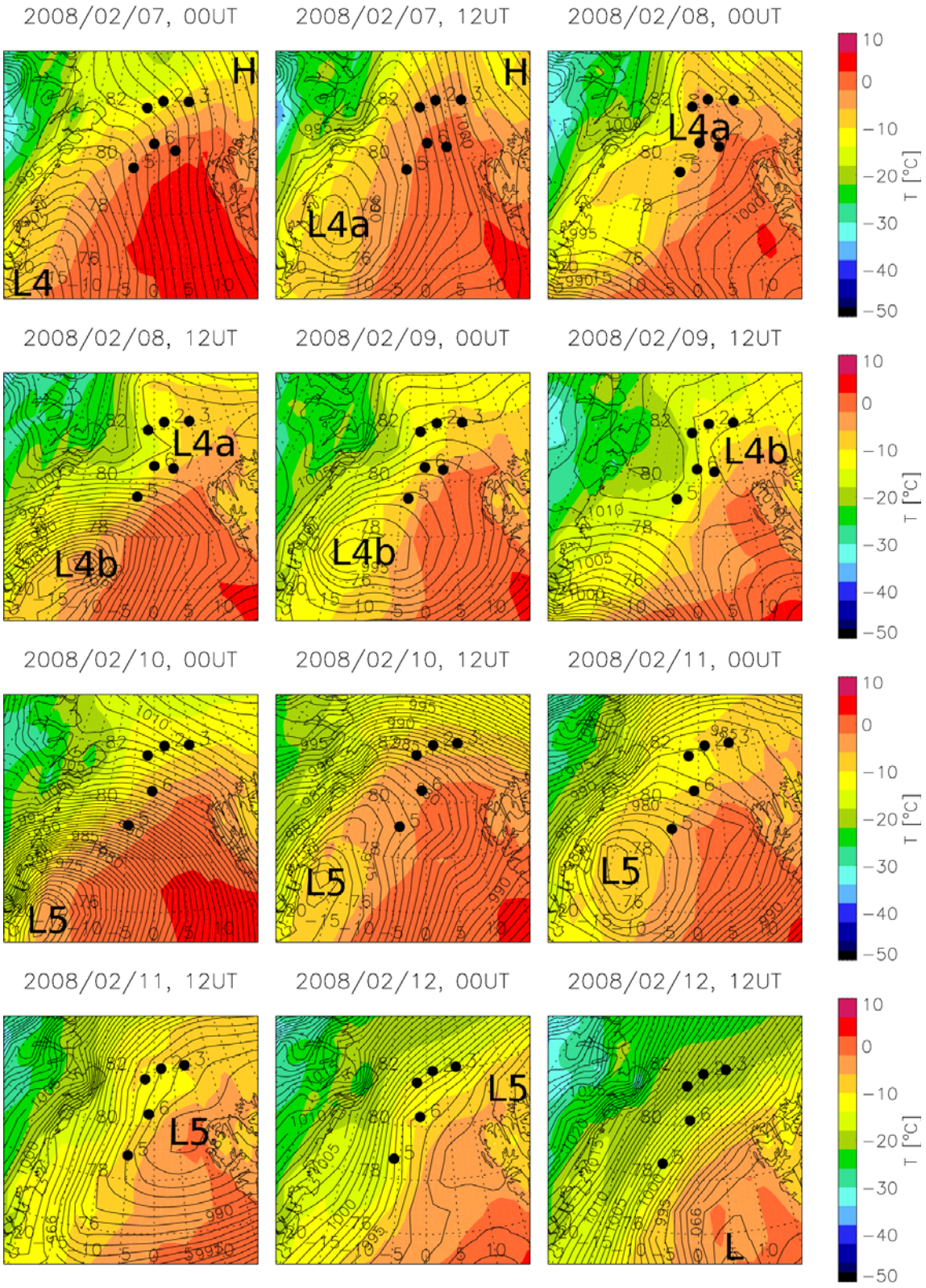
2008/02/07, 00UT
2008/02/07, 12UT
2008/02/08, 00UT
2008/02/08, 12UT
2008/02/09, 00UT
2008/02/09, 12UT
2008/02/10, 00UT
2008/02/10, 12UT
2008/02/11, 00UT
2008/02/11, 12UT
2008/02/12, 00UT
2008/02/12, 12UT
H
L4
L4a
L4b
L5
L
T [°C]
10
0
−10
−20
−30
−40
−50

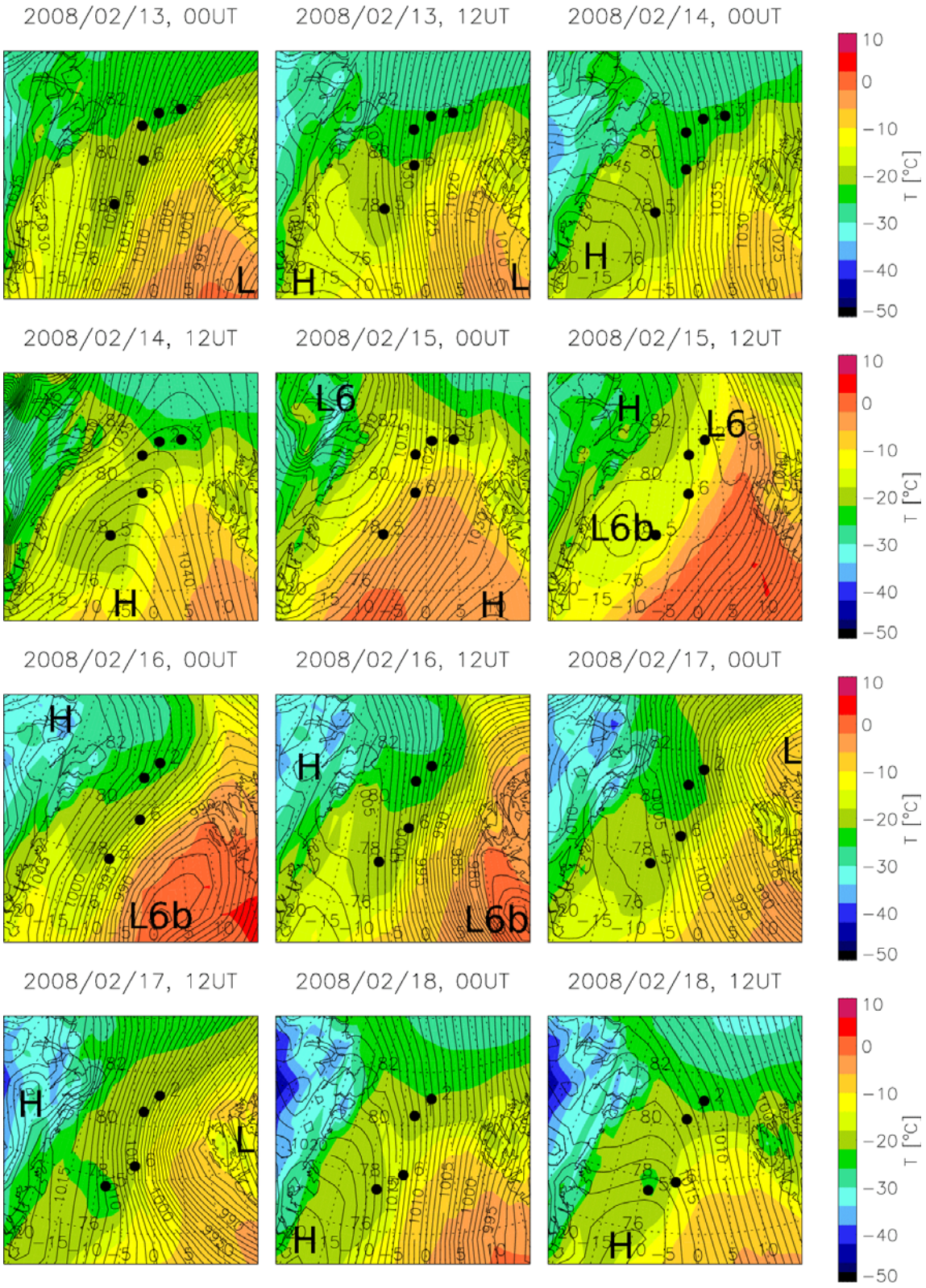
2008/02/13, 00UT
2008/02/13, 12UT
2008/02/14, 00UT
2008/02/14, 12UT
2008/02/15, 00UT
2008/02/15, 12UT
2008/02/16, 00UT
2008/02/16, 12UT
2008/02/17, 00UT
2008/02/17, 12UT
2008/02/18, 00UT
2008/02/18, 12UT
H
L
L6
L6b
T [°C]
10
0
−10
−20
−30
−40
−50

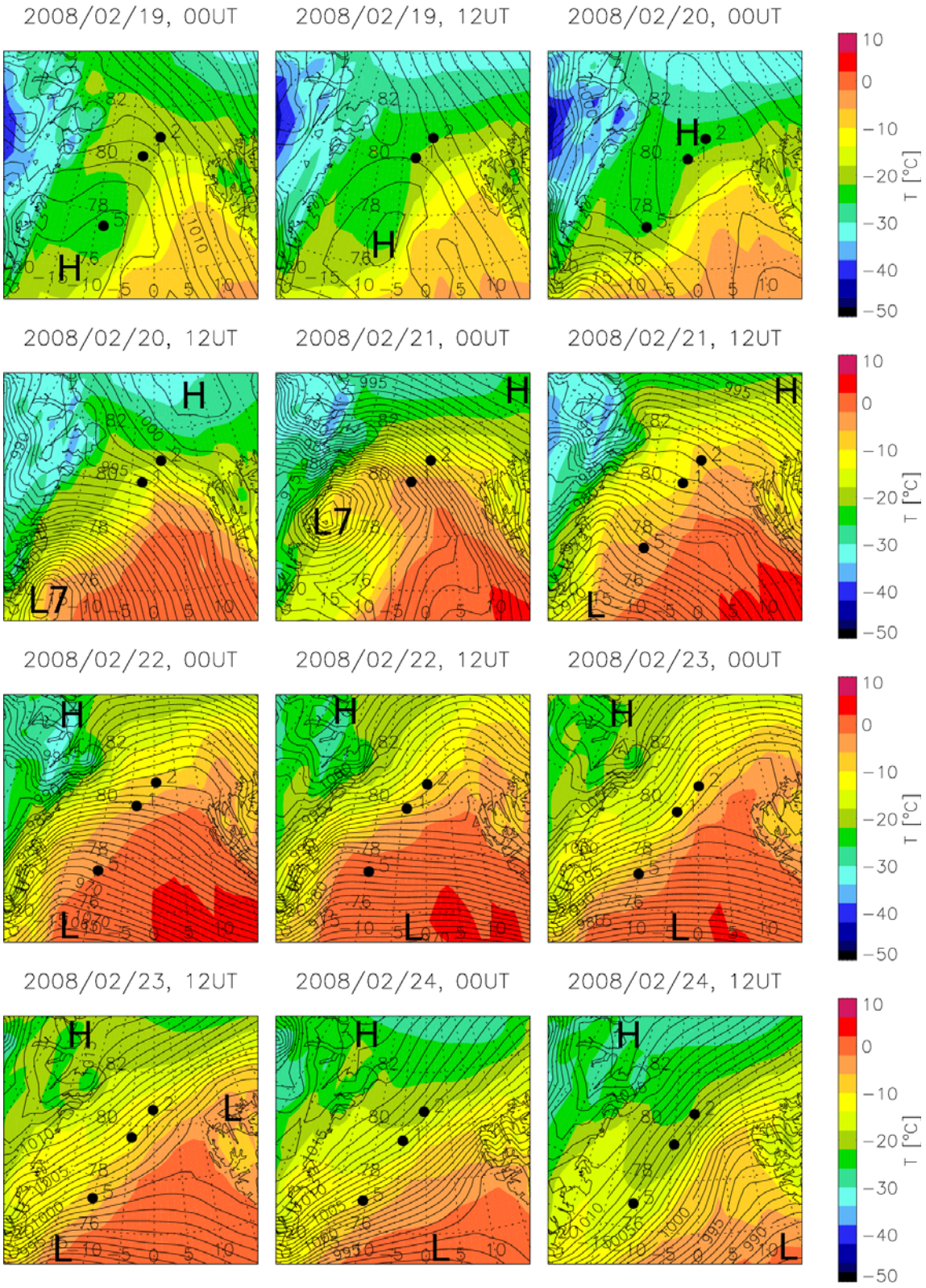
2008/02/19, 00UT
2008/02/19, 12UT
2008/02/20, 00UT
2008/02/20, 12UT
2008/02/21, 00UT
2008/02/21, 12UT
2008/02/22, 00UT
2008/02/22, 12UT
2008/02/23, 00UT
2008/02/23, 12UT
2008/02/24, 00UT
2008/02/24, 12UT
T [°C]
10
0
−10
−20
−30
−40
−50

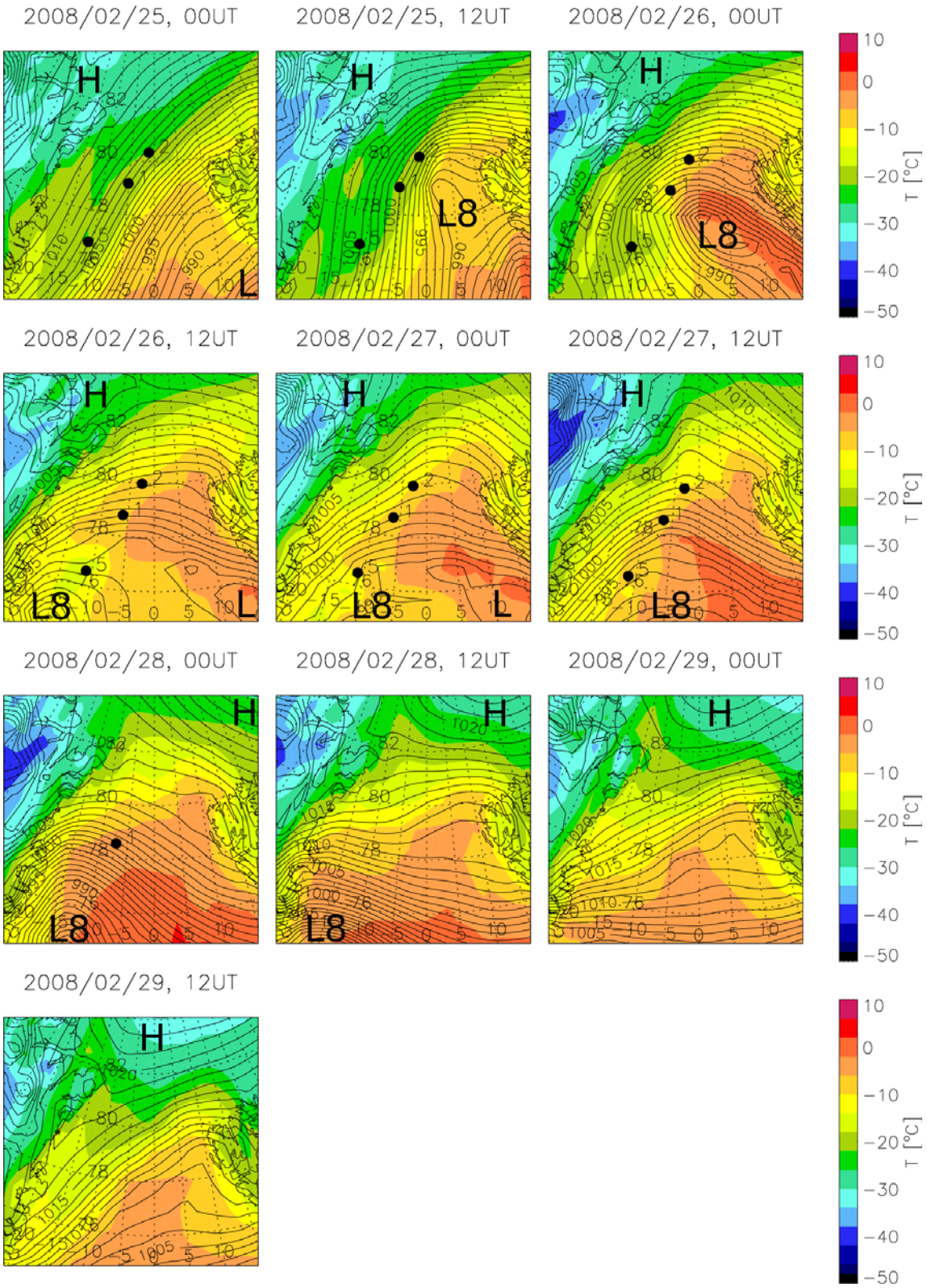
2008/02/25, 00UT
2008/02/25, 12UT
2008/02/26, 00UT
2008/02/26, 12UT
2008/02/27, 00UT
2008/02/27, 12UT
2008/02/28, 00UT
2008/02/28, 12UT
2008/02/29, 00UT
2008/02/29, 12UT
H
L
L8
T [°C]
10
0
−10
−20
−30
−40
−50

A2 Ice concentration and extent from SSM/I and NOAA

Appendix A2 lists daily maps of sea ice concentration provided by Lars Kaleschke from the Institut für Meereskunde at the University of Hamburg. Sea ice concentration is retrieved from the 59 GHT channels of the AMSR-E (Advanced Microwave Scanning Radiometer) instrument on the AQUA satellite applying the ASI algorithm (e.g. Spreen et al., 2008). Black dots mark the positions of the CALIB buoys.

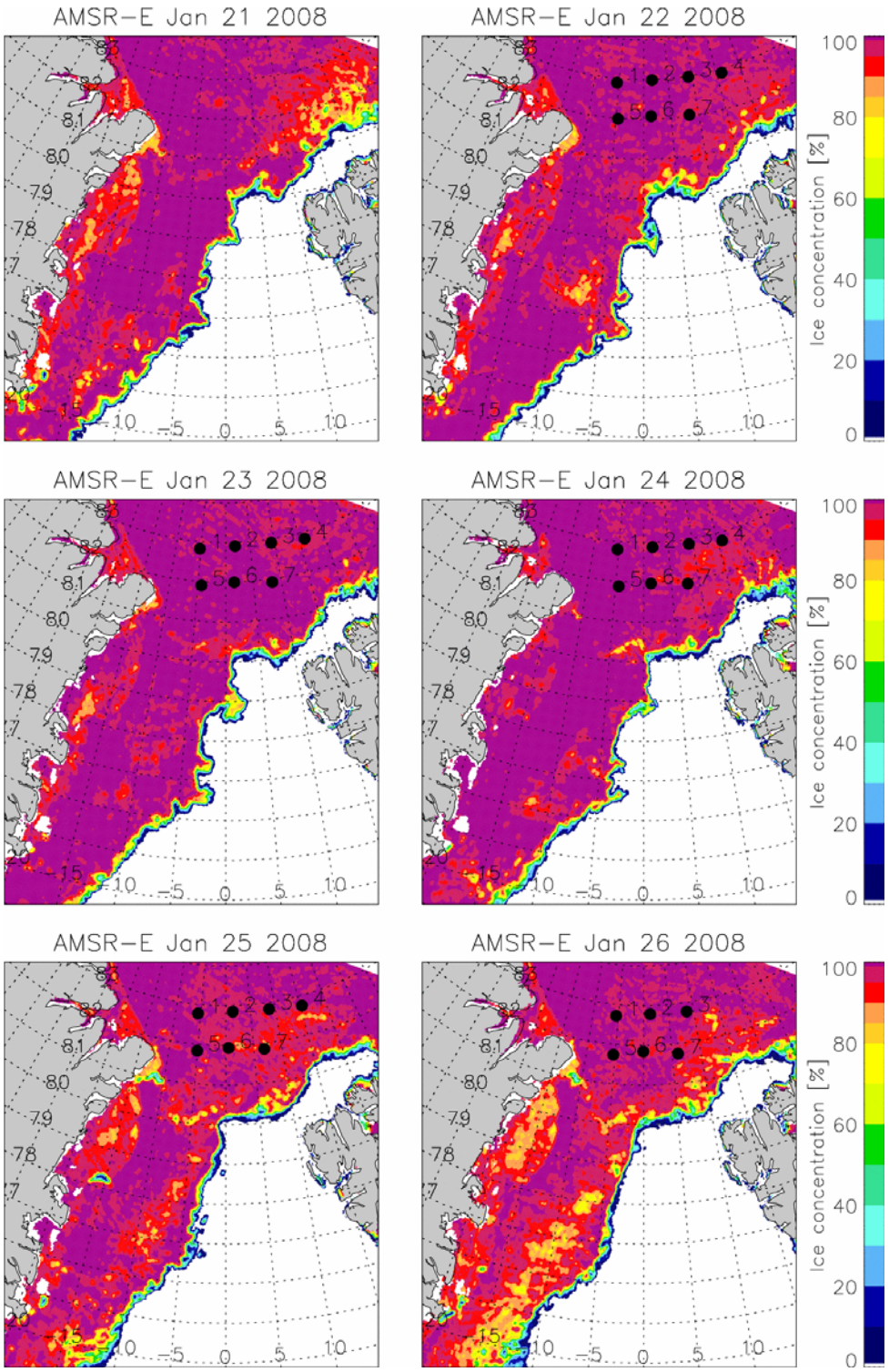

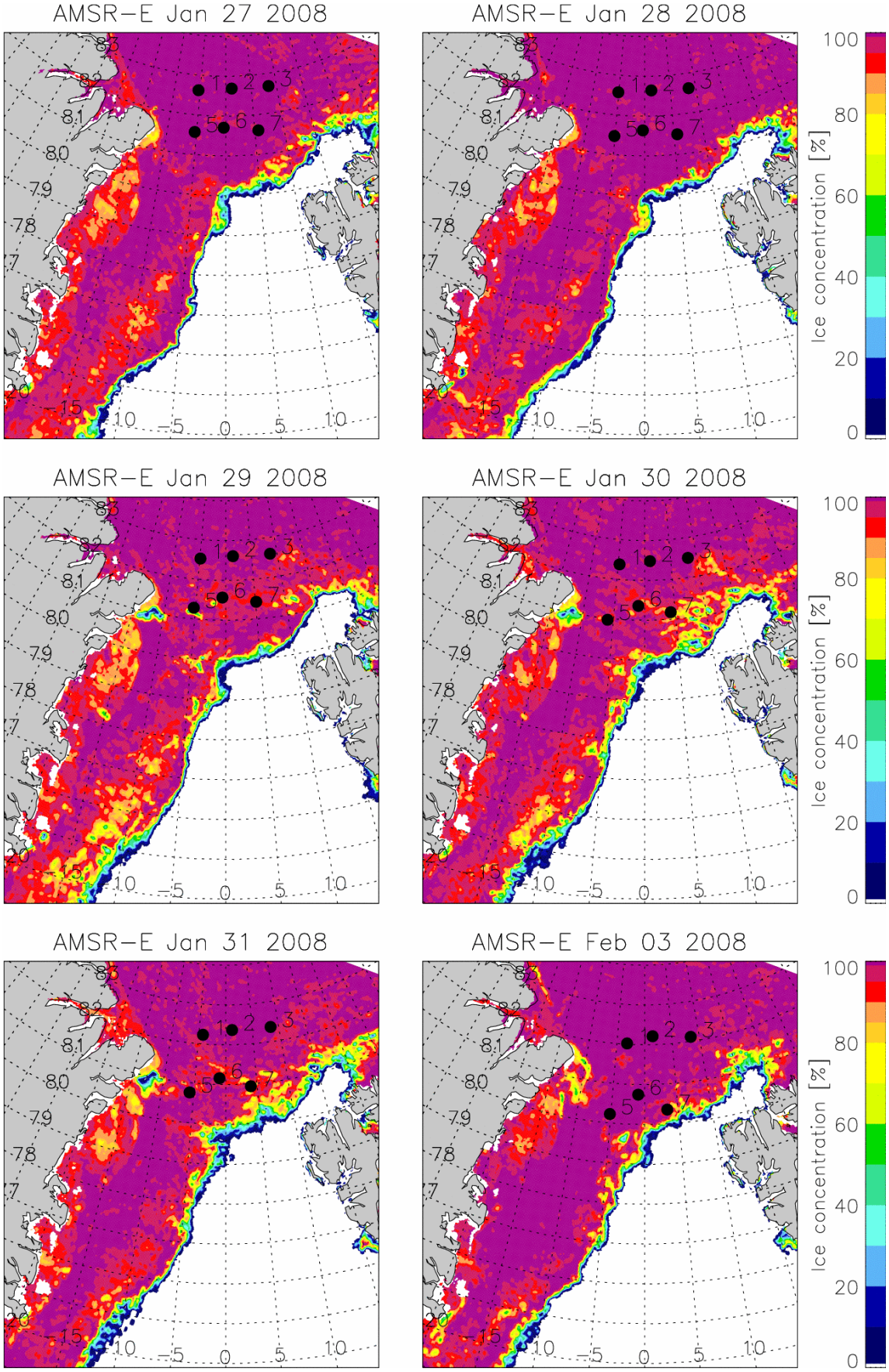
AMSR−E Jan 27 2008
AMSR−E Jan 28 2008
AMSR−E Jan 29 2008
AMSR−E Jan 30 2008
AMSR−E Jan 31 2008
AMSR−E Feb 03 2008
Ice concentration [%]
100
80
60
40
20
0

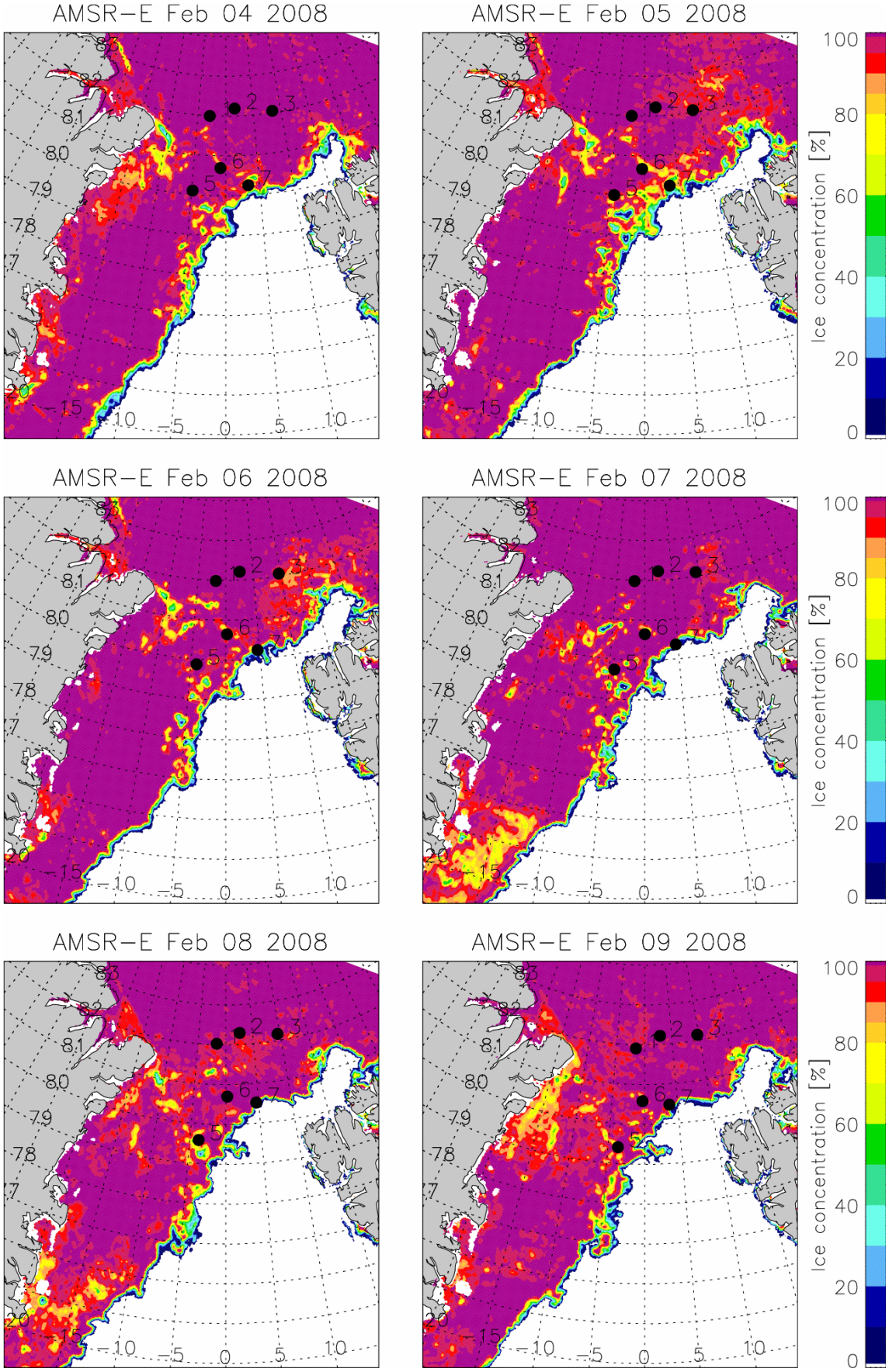
AMSR−E Feb 04 2008
AMSR−E Feb 05 2008
AMSR−E Feb 06 2008
AMSR−E Feb 07 2008
AMSR−E Feb 08 2008
AMSR−E Feb 09 2008
Ice concentration [%]
100
80
60
40
20
0

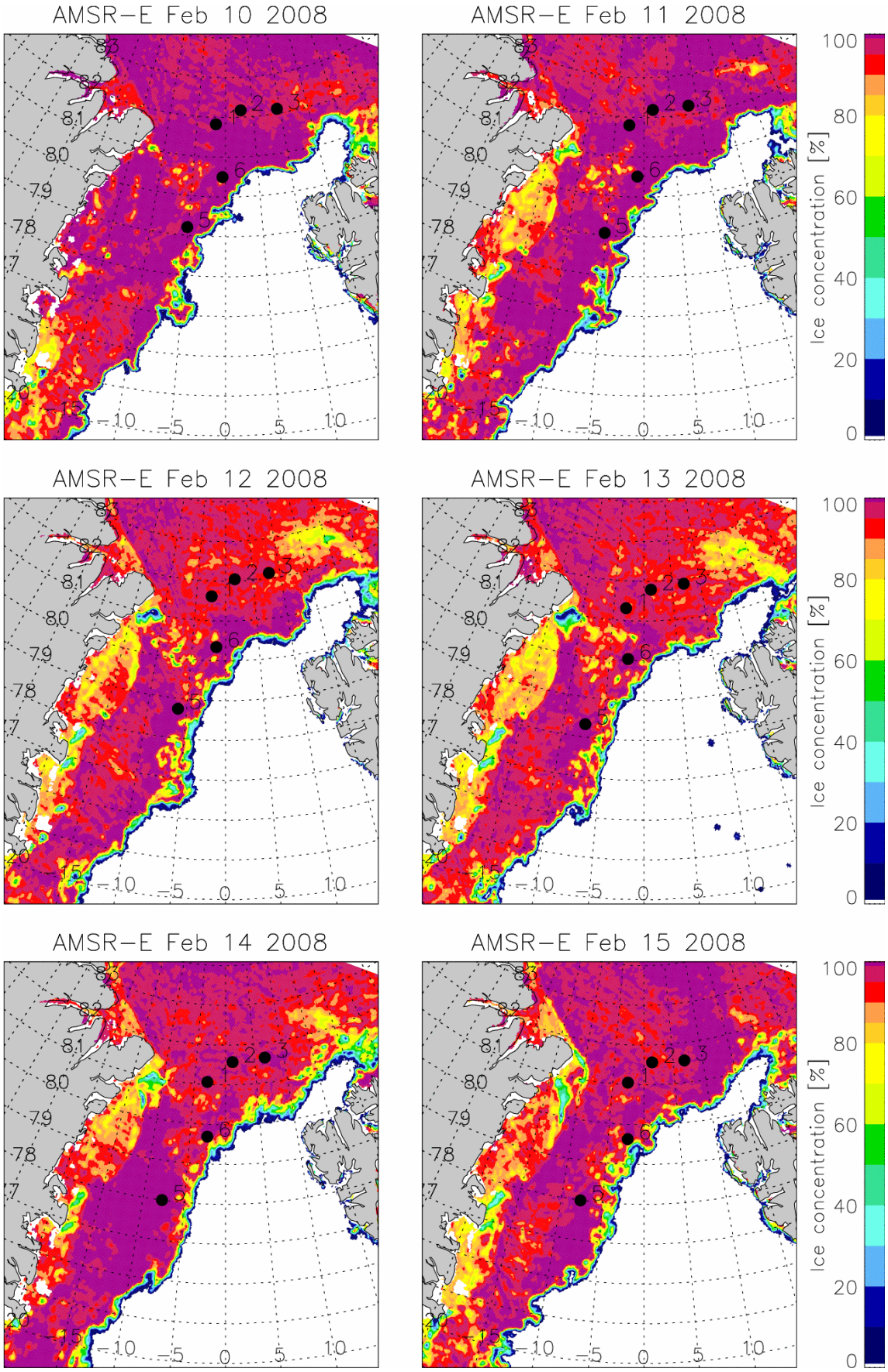
AMSR−E Feb 10 2008
AMSR−E Feb 11 2008
AMSR−E Feb 12 2008
AMSR−E Feb 13 2008
AMSR−E Feb 14 2008
AMSR−E Feb 15 2008
Ice concentration [%]
100
80
60
40
20
0
1
2
3
5
6
83
82
81
80
79
78
7
−10
−5
0
5
10
15
20

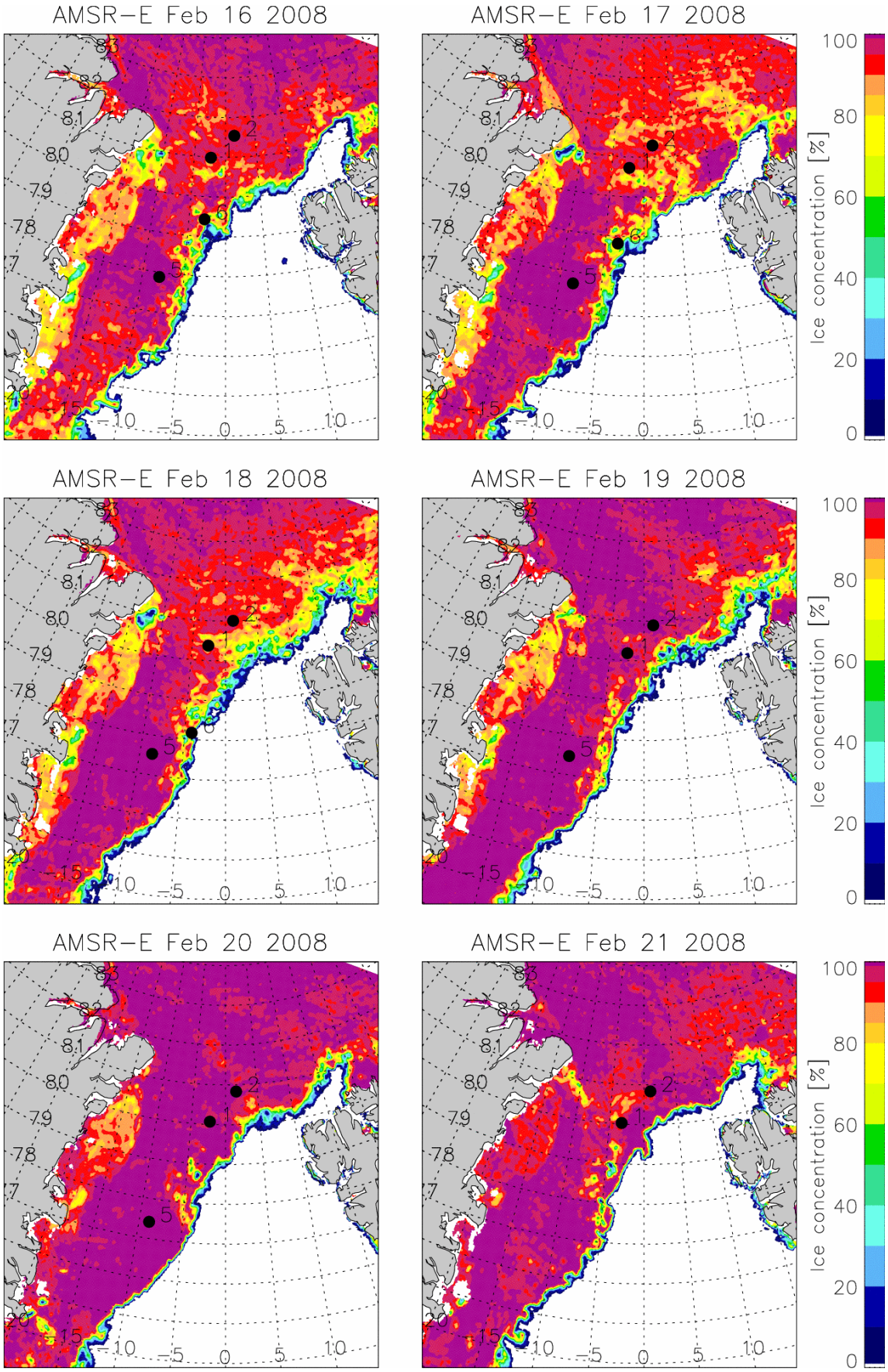
AMSR−E Feb 16 2008
AMSR−E Feb 17 2008
AMSR−E Feb 18 2008
AMSR−E Feb 19 2008
AMSR−E Feb 20 2008
AMSR−E Feb 21 2008
Ice concentration [%]
100
80
60
40
20
0
1
2
3
5
6
8.3
8.2
8.1
8.0
7.9
7.8
7
20
15
−10
−5
0
5
10

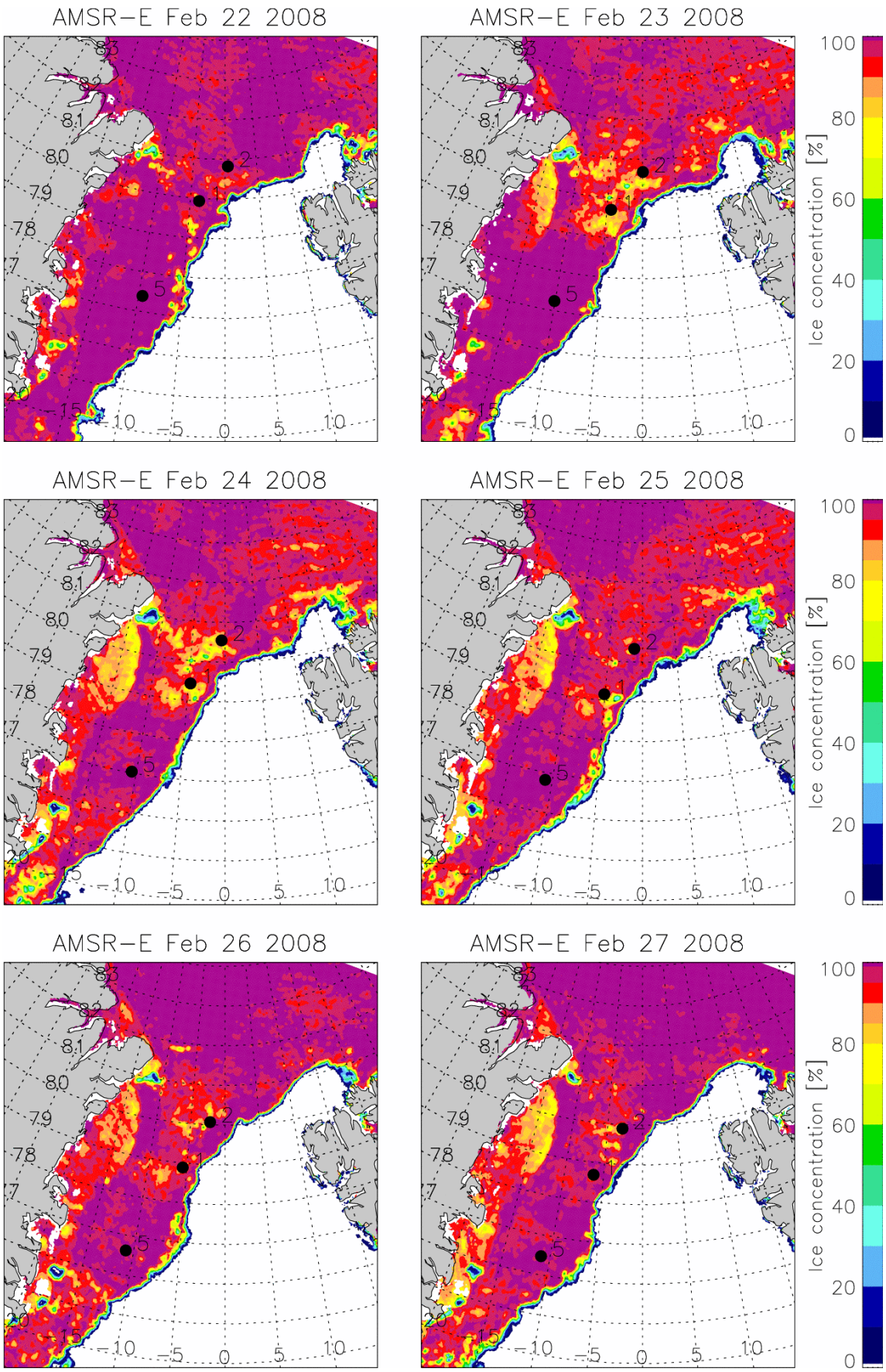
AMSR−E Feb 22 2008
AMSR−E Feb 23 2008
AMSR−E Feb 24 2008
AMSR−E Feb 25 2008
AMSR−E Feb 26 2008
AMSR−E Feb 27 2008
Ice concentration [%]
100
80
60
40
20
0
83
82
81
80
79
78
7
−15
−10
−5
0
5
10
1
2
5

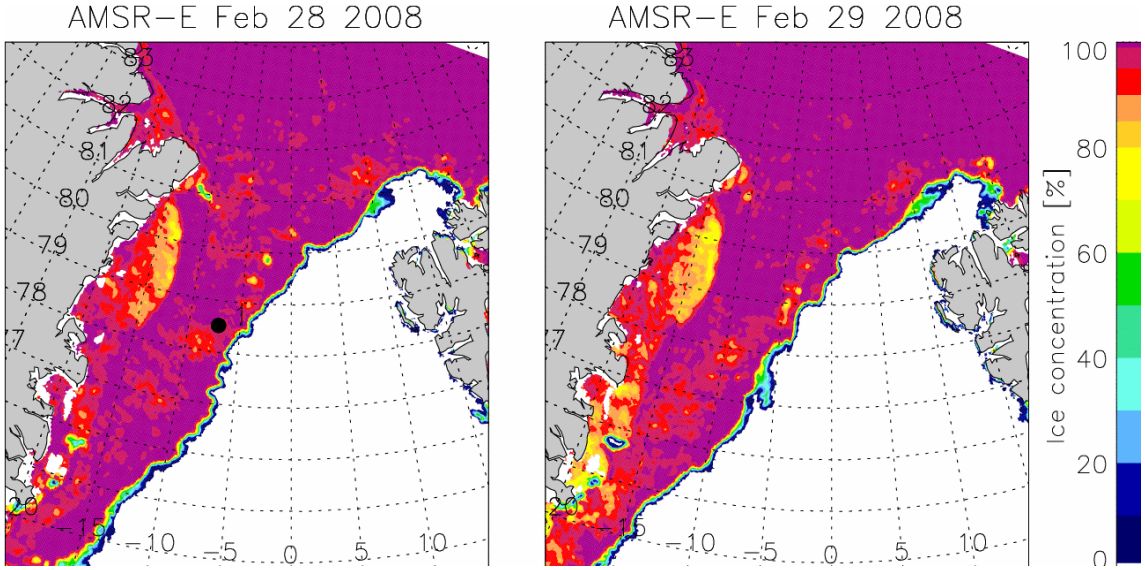
AMSR−E Feb 28 2008
AMSR−E Feb 29 2008
8.3
8.2
8.1
8.0
7.9
7.8
7.7
−15
−10
−5
0
5
10
100
80
60
40
20
0
Ice concentration [%]

A3 NOAA satellite images

Appendix A3 lists daily NOAA satellite images (around noon UTC) in the infrared channel CH4. The images were taken with courtesy of Bernard Burton from the Wokingham Weather webpage: www.btinternet.com/~wokingham.weather/wwp.html. Crosses mark the actual positions of the CALIB ice buoys.

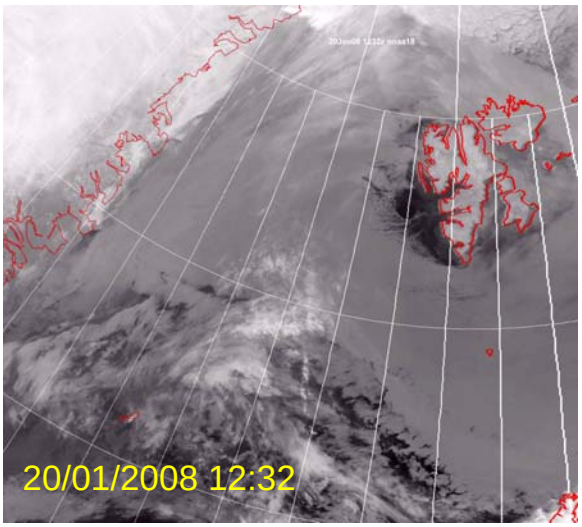

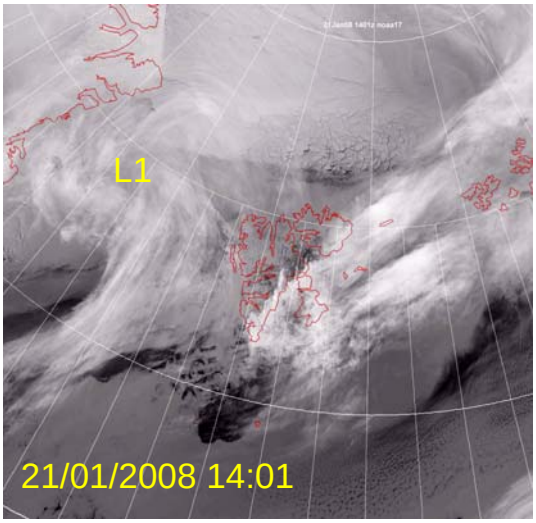

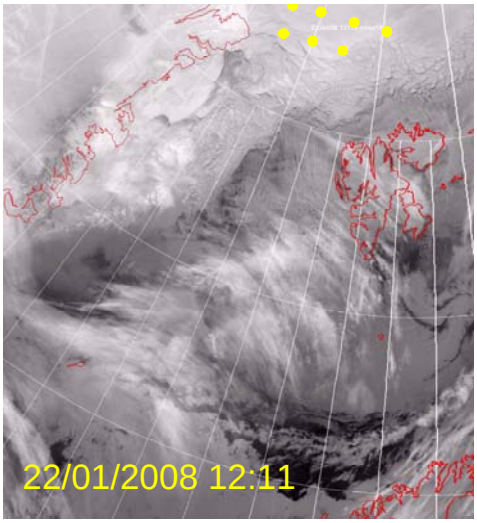

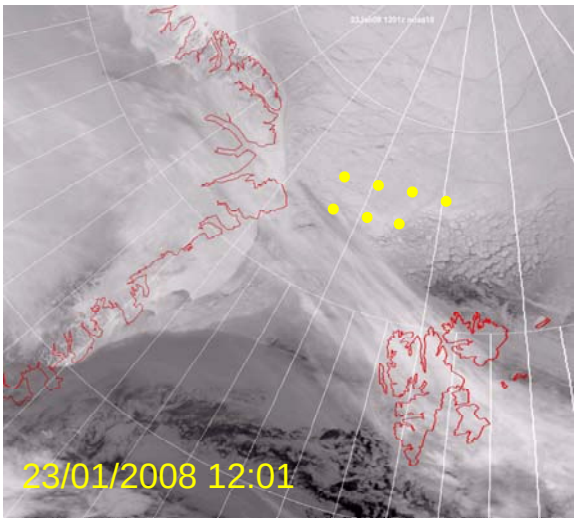

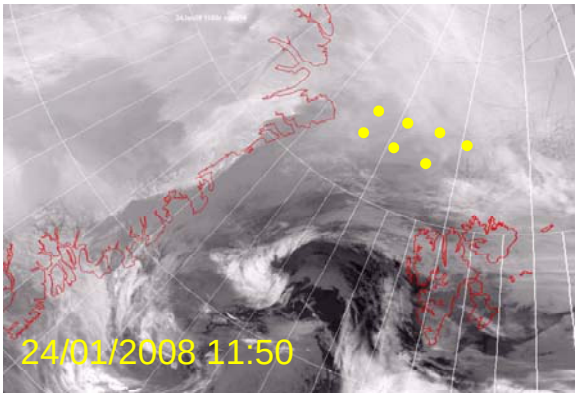
24/01/2008 11:50

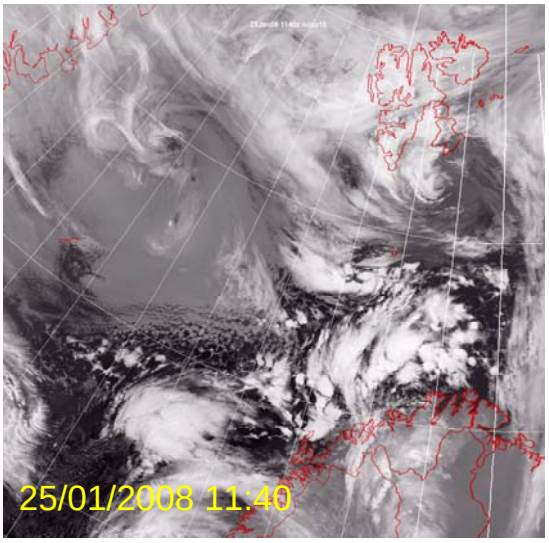
25/01/2008 11:40

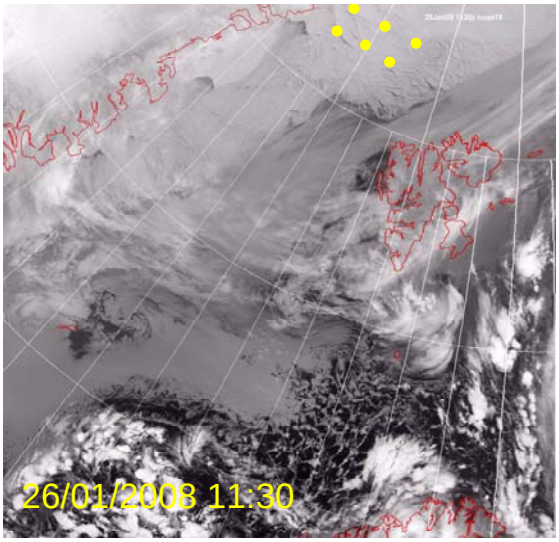
26/01/2008 11:30

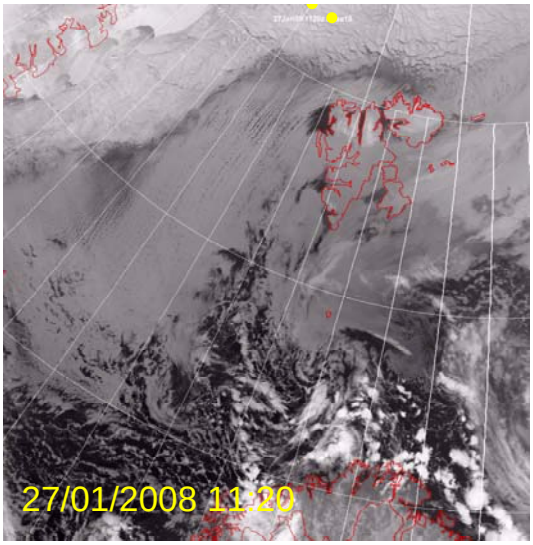
27/01/2008 11:20

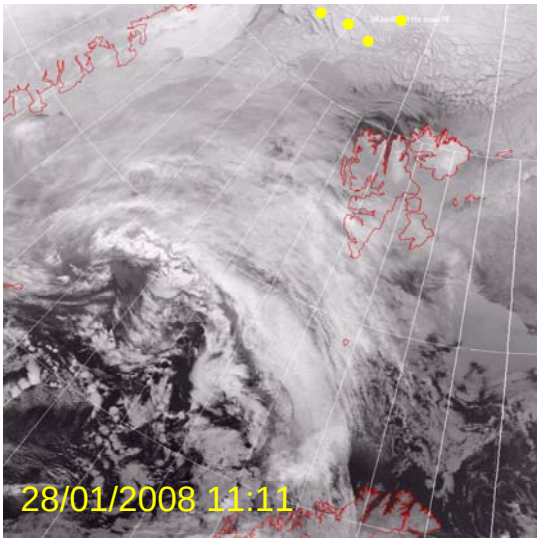
28/01/2008 11:11

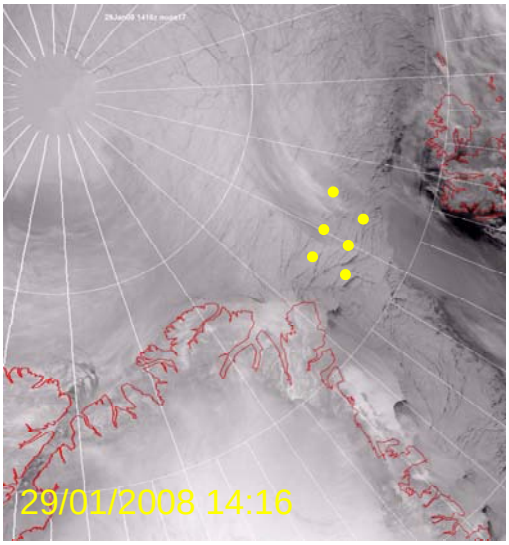
29/01/2008 14:16

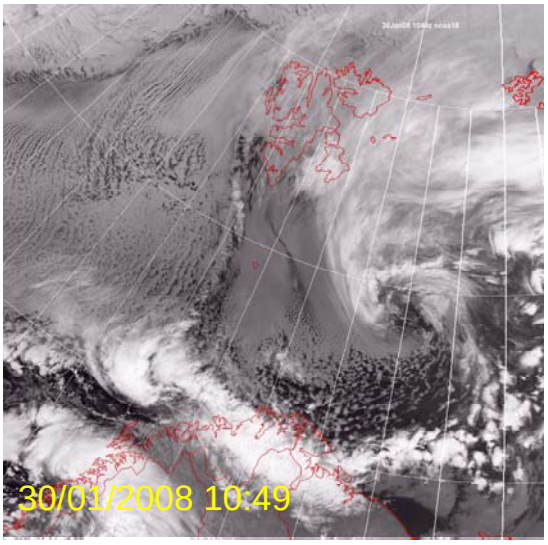
30/01/2008 10:49

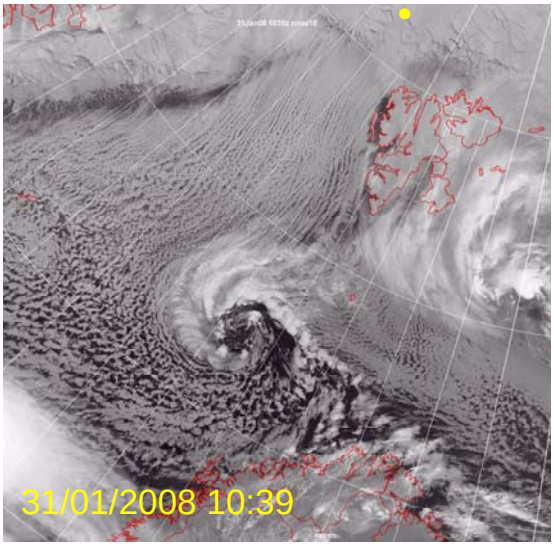
31/01/2008 10:39

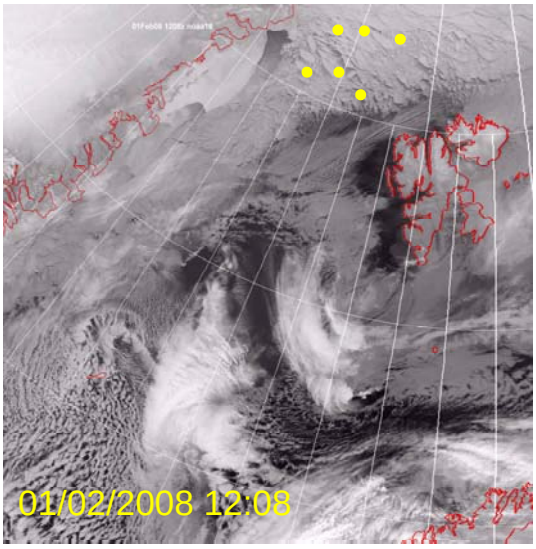
01/02/2008 12:08

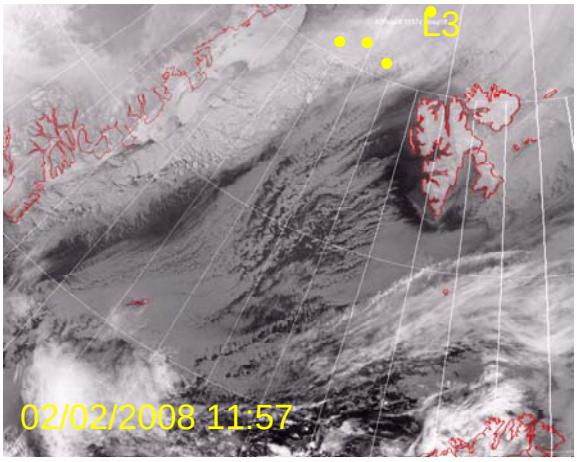
L3
02/02/2008 11:57

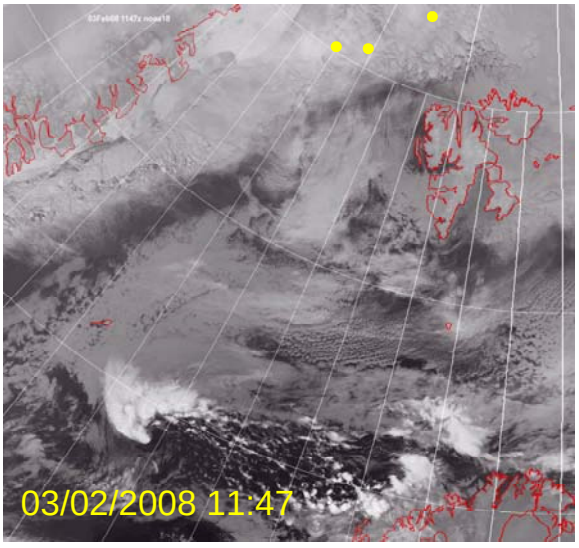
03/02/2008 11:47

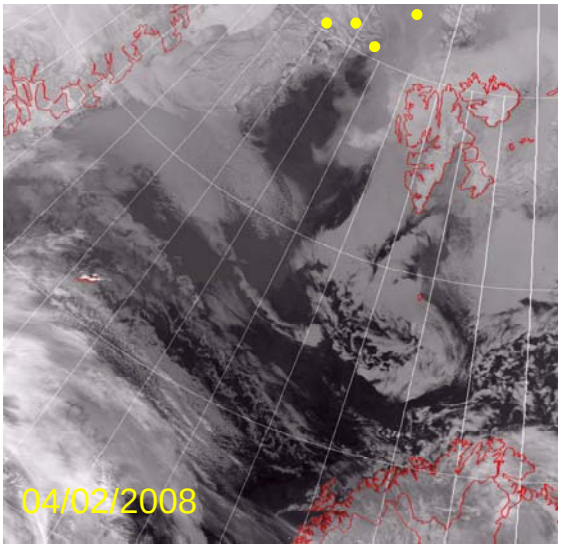
04/02/2008

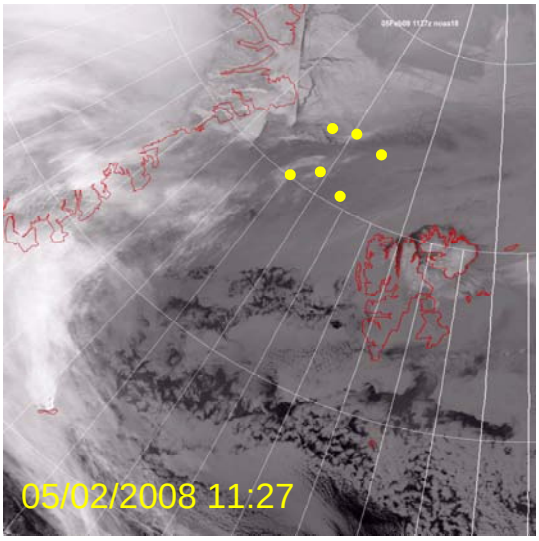
05/02/2008 11:27

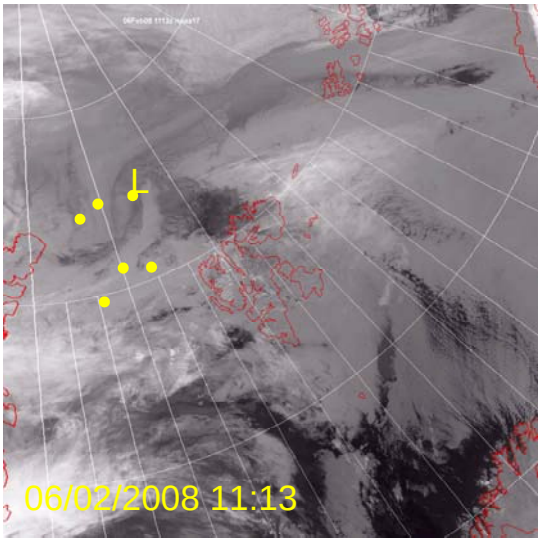
L
06/02/2008 11:13

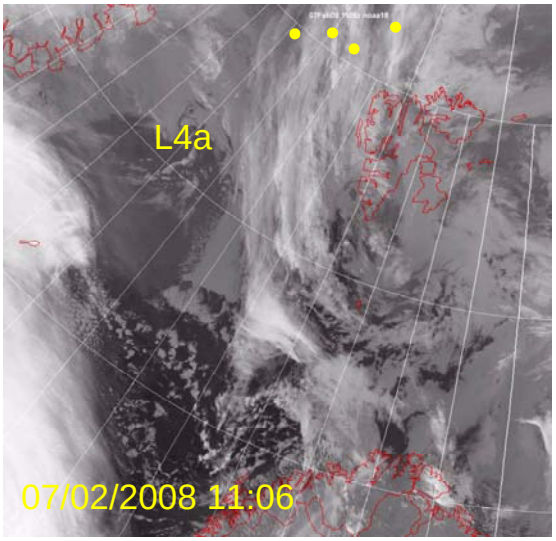
L4a
07/02/2008 11:06

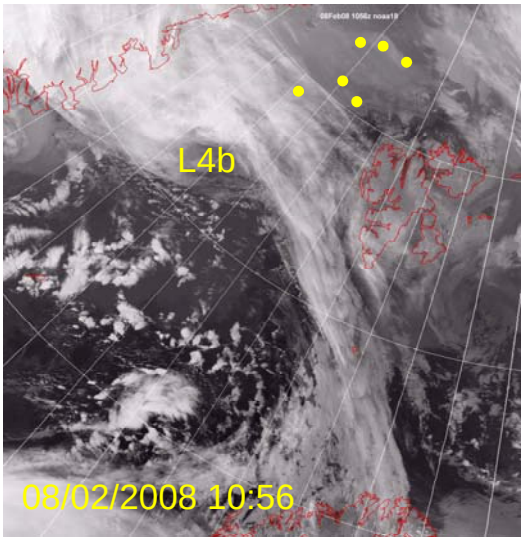
L4b
08/02/2008 10:56

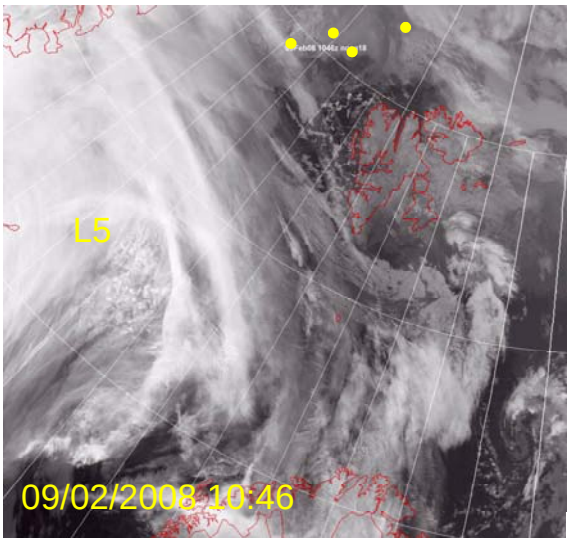
L5
09/02/2008 10:46

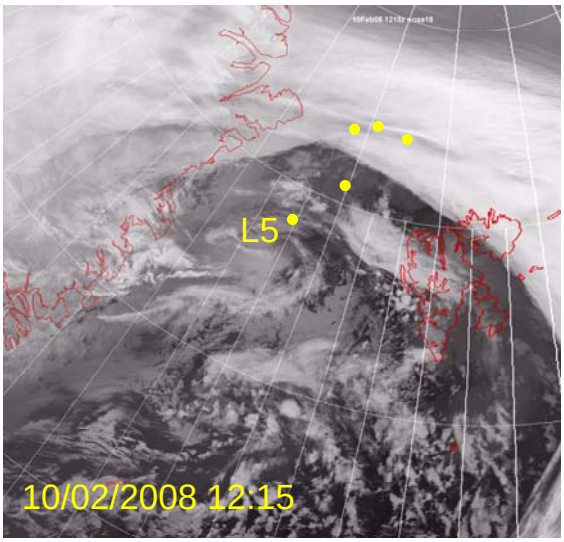
L5
10/02/2008 12:15

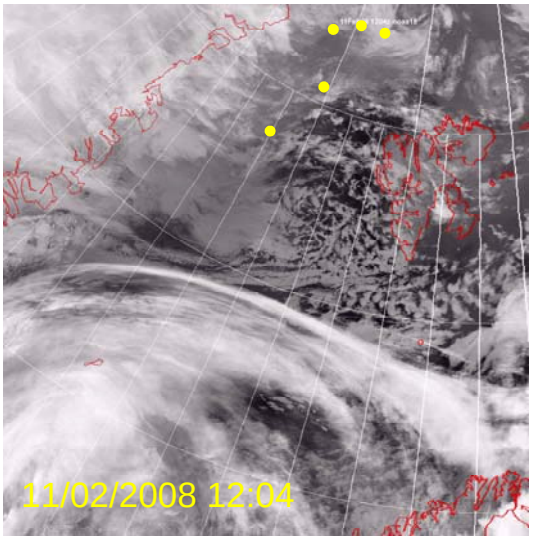
11/02/2008 12:04

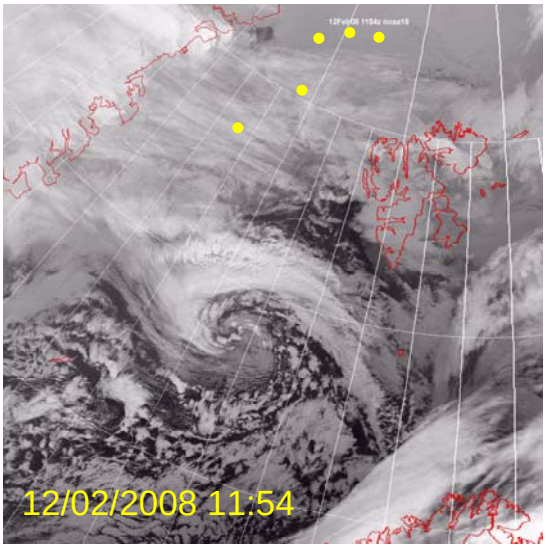
12/02/2008 11:54

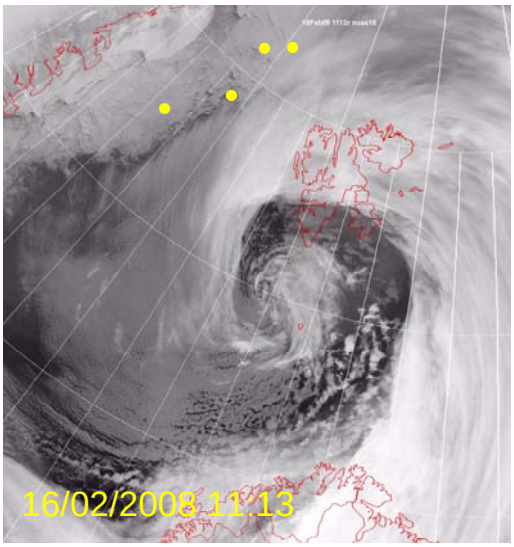
16/02/2008 11:13

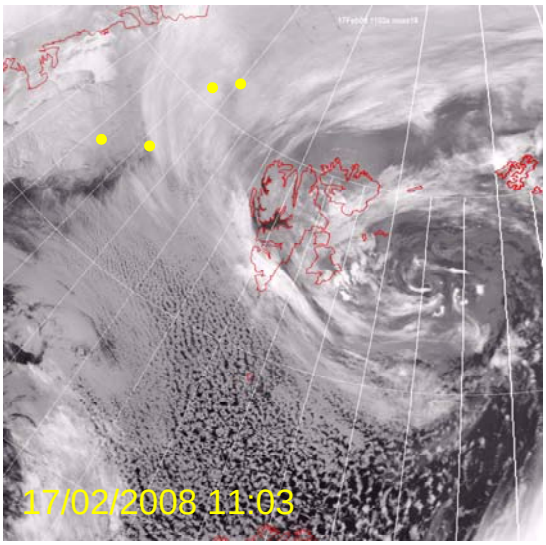
17/02/2008 11:03

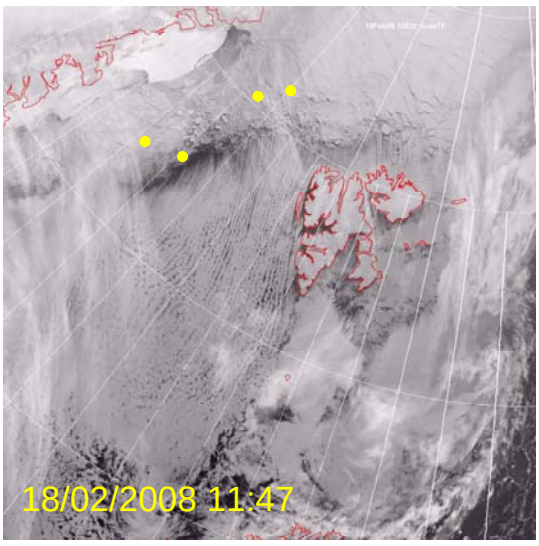
18/02/2008 11:47

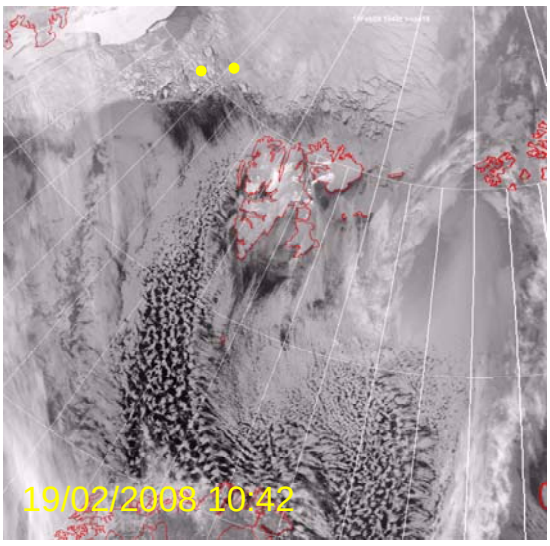
19/02/2008 10:42

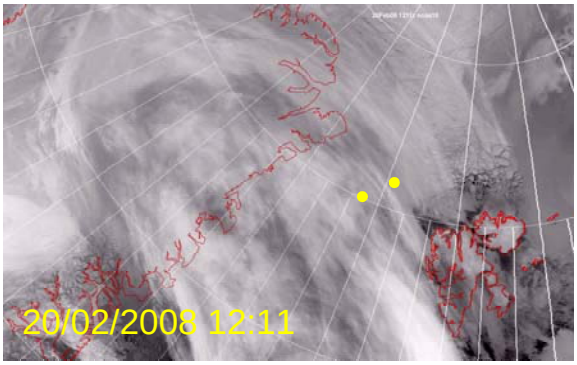
20/02/2008 12:11

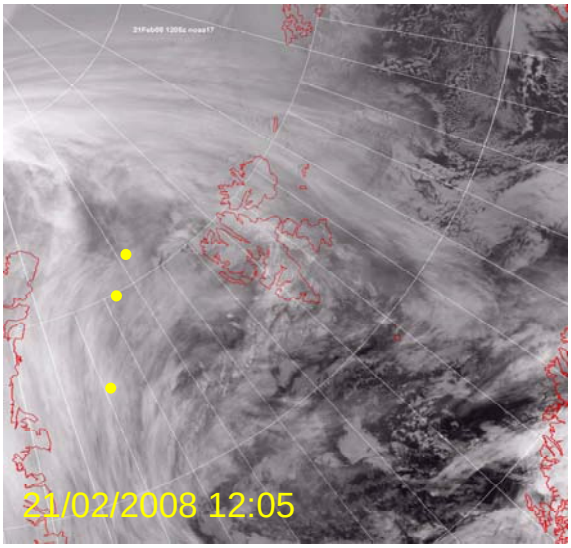
21/02/2008 12:05

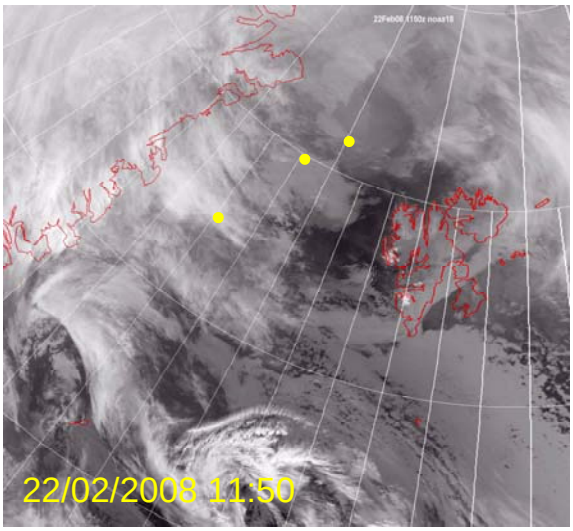
22/02/2008 11:50

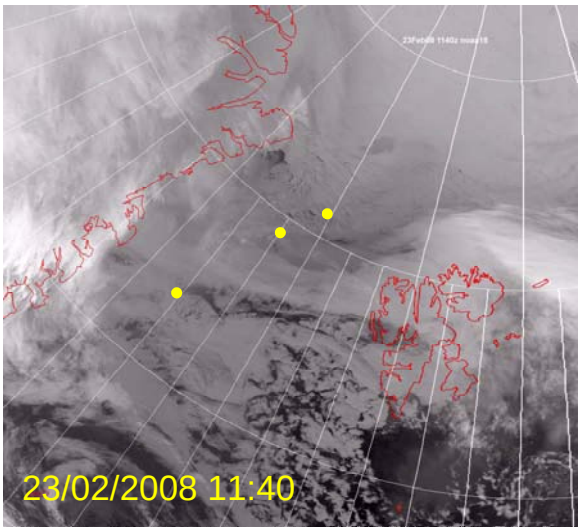
23/02/2008 11:40

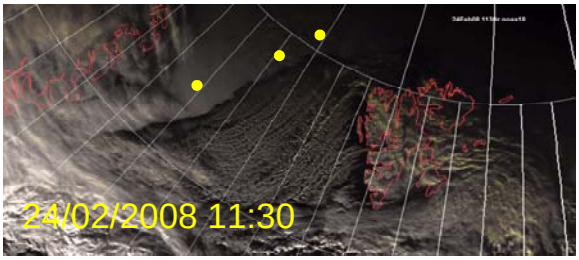
24/02/2008 11:30

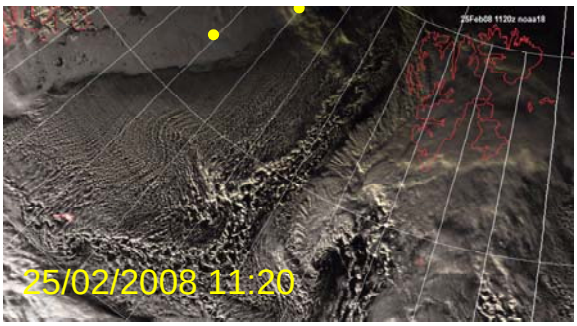
25/02/2008 11:20

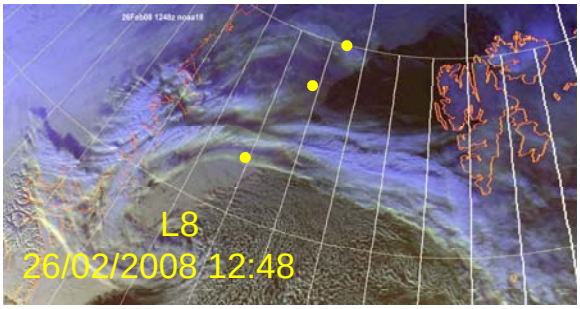
L8
26/02/2008 12:48

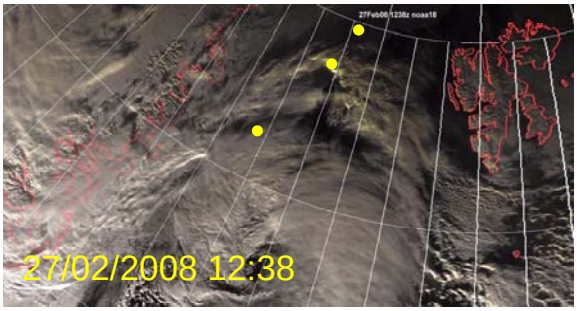
27/02/2008 12:38

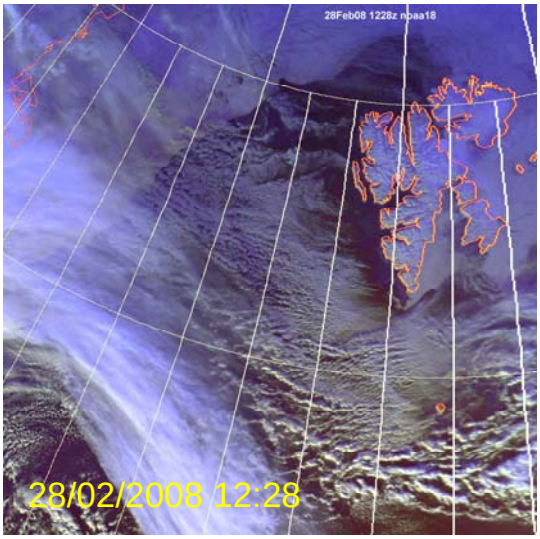
28Feb08 1228z noaa18
28/02/2008 12:28

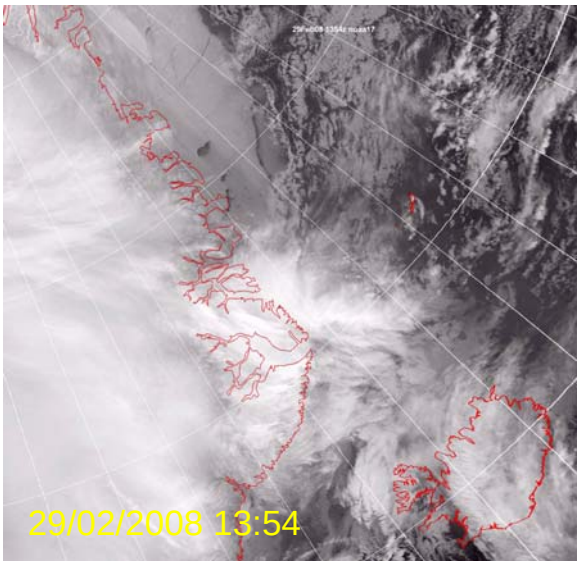
29/02/2008 13:54

Berichte aus dem Zentrum für Meeres- und Klimaforschung - Reihe A

Meteorologisches Institut
Bundesstr. 55
20146 Hamburg http://www.mi.uni-hamburg.de

1. Schlüssel, P. ; Taurat, D. (1992): The benefits from a synergy of passive satellite measurements with active LIDAR soundings.

2. Brinkop, S. (1992): Parameterisierung von Grenzschichtwolken für Zirkulationsmodelle.

3. Brümmer, B. [Hrsg.] (1992): ARKTIS 1991- Report on the field phase with examples of measurements.

4. Schulz, J. (1993): Fernerkundung des latenten Wärmeflusses an der Meeresoberfläche.

5. Nodorp, D. (1993): Ein Zirkulationsmodell mit transientem Antrieb.

6. Marotzke, K. (1993): Physikalische Modellierung der Ausbreitung störfallartig freigesetzter schwerer Gase zur Abschätzung von Gefahrenbereichen im bebauten Gelände.

7. Martin, T. (1993): Multispektrale Meereisklassifikation mit passiven Satellitenradiometern.

8. Lunkeit, F. (1993): Simulation der interannualen Variabilität mit einem globalen gekoppelten Atmosphäre-Ozean Modell.

9. Kollewe, M. (1993): Fernerkundung von Wolken mit der Sauerstoff Absorptionsbande im nahen Infrarot.

10. Standfuss, C.; Hollweg, H.-D.; Graßl, H. (1993): The impact of a Radiation Budget Scanner aboard Meteosat second generation on the accuracy of regional budget parameters.

11. Brümmer, B. [Hrsg.] (1993): ARKTIS 1993- Report on the field phase with examples of measurements.

12. Richter, M.C. (1994): Niederschlagsmessung mit dem vertikal ausgerichteten FM-CW-Doppler-Radar-RASS-System - Validierung und Anwendung.

13. Festschrift zum 70. Geburtstag von Prof. Dr. G. Fischer (1994).

14. Khvorostyanov, V.I. (1994): Mesoscale processes of cloud formation, cloud radiation interaction, and their modelling with explicit cloud microphysics.

15. Wyputta, U. (1994): Untersuchungen zum Stofftransport in die Antarktis anhand von Messungen an der Georg-von-Neumayer-Station.

16. Müller, G. (1995): Mesoskalige Zellularkonvektion in Abhängigkeit von unterschiedlichen physikalischen Prozessen und synoptischen Randbedingungen - Numerische Simulationen.

17. Hollweg, H.-D. et al (1995): Interaction at mm and optical frequencies. Part I: Current problems in radiative transfer simulations.

18. Hollweg, H.-D. et al (1995): Interactions at mm and optical frequencies. Part II: Specific atmospheric absorption and emission features: Investigation and modelling.

19. Grötzner, A. (1995): Subskalige partielle Meereisbedeckung in einem globalen atmosphärischen Zirkulationsmodell.

20. Schlüssel, P. (1995): Passive Fernerkundung der unteren Atmosphäre und der Meeresoberfläche aus dem Weltraum.

21. Bartsch, B. (1996): Fernerkundung des Wasserdampfgehalts der Atmosphäre über Land aus rückgestreuter Sonnenstrahlung.

22. Taurat, D. (1996): Windfelder über See unter Verwendung von Satellitendaten und Druckanalysen.

23. Schlünzen, K.H. (1996): Validierung hochauflösender Regionalmodelle.

24. Donat, J. (1996): Windkanalexperimente zur Ausbreitung von Schwergasstrahlen.

25. Roth, B. (1996): Bildung von H2SO4-H2O-Aerosol in einem vertikalen lamiaren Strömungsreaktor.

26. Thiemann, S. (1996): Die vertikale Struktur der konvektiven Grenzschicht während arktischer Kaltluftausbrüche über See.

27. Standfuss, C. et al (1996): Earth Radiation Budget - General Purpose Data Base.

28. Niemeier, U. (1997): Chemische Umsetzungen in einem hochauflösenden mesoskaligen Modell.

29. Schneider, W. (1997): Die Nordostwasser Polynja: Entstehung und Hydrographie.

30. v. Salzen, K. (1997): Entwicklung und Anwendung eines Modells für die Dynamik und Zusammensetzung sekundären und marinen Aerosols.

31. Klugmann, D. (1998): Messung von Niederschlag und Vertikalwind in der unteren Atmosphäre mit Millimeterwellen-Doppler-RADAR-Profilern.

32. Brümmer, B. and S. Thiemann (1999): Field Campaign ACSYS 1998: Aircraft measurements in Arctic on-ice air flows.

33. Brümmer, B. (2000): Field experiment FRAMZY 1999 - Cyclones over the Fram Strait and their impact on sea ice. Field report with examples of measurements.

34. Ganske, A., G. Peters und B. Fischer (2002): Bestimmung meteorologischer Ausbreitungsparameter mit SODAR.

35. Dierer, S. (2002): Untersuchung von groß- und mesoskaligen Einflüssen auf die Entwicklung polarer Mesozyklonen mit Hilfe des Modells METRAS.

36. Schimmel, F. (2002): Development and test of an atmospheric flow model employing adaptive numerical methods.

37. Brümmer, B. et al (2005): FRAMZY 2002 – Second field experiment on Fram Strait cyclones and their impact on sea ice. Field report with measurement examples.

38. Meyer, E. M. I. (2006): Die Bedeutung atmosphärischer Prozesse für den Stickstoffeintrag in Küstengewässer.

39. Schlüter, I. (2006): Simulation des Transports biogener Emissionen in und über einem Waldbestand mit einem mikroskaligen Modellsystem.

40. Brümmer, B. et al (2009): The drift buoys experiment: FRAMZY 2009 - Ice drift in Fram Strait and relation to atmospheric forcing.